DAVID W. TAYLOR NAVAL SHIP RESEARCH AND DEVELOPMENT CENTER

Bethesda, Md. 20084

THEORETICAL DETERMINATION OF PORPOISING INSTABILITY OF HIGH-SPEED PLANING BOATS

by

Milton Martin

APPROVED FOR PUBLIC RELEASE: DISTRIBUTION UNLIMITED

SHIP PERFORMANCE DEPARTMENT
RESEARCH AND DEVELOPMENT REPORT

April 1976

Report 76-0068

MAJOR DTNSRDC ORGANIZATIONAL COMPONENTS

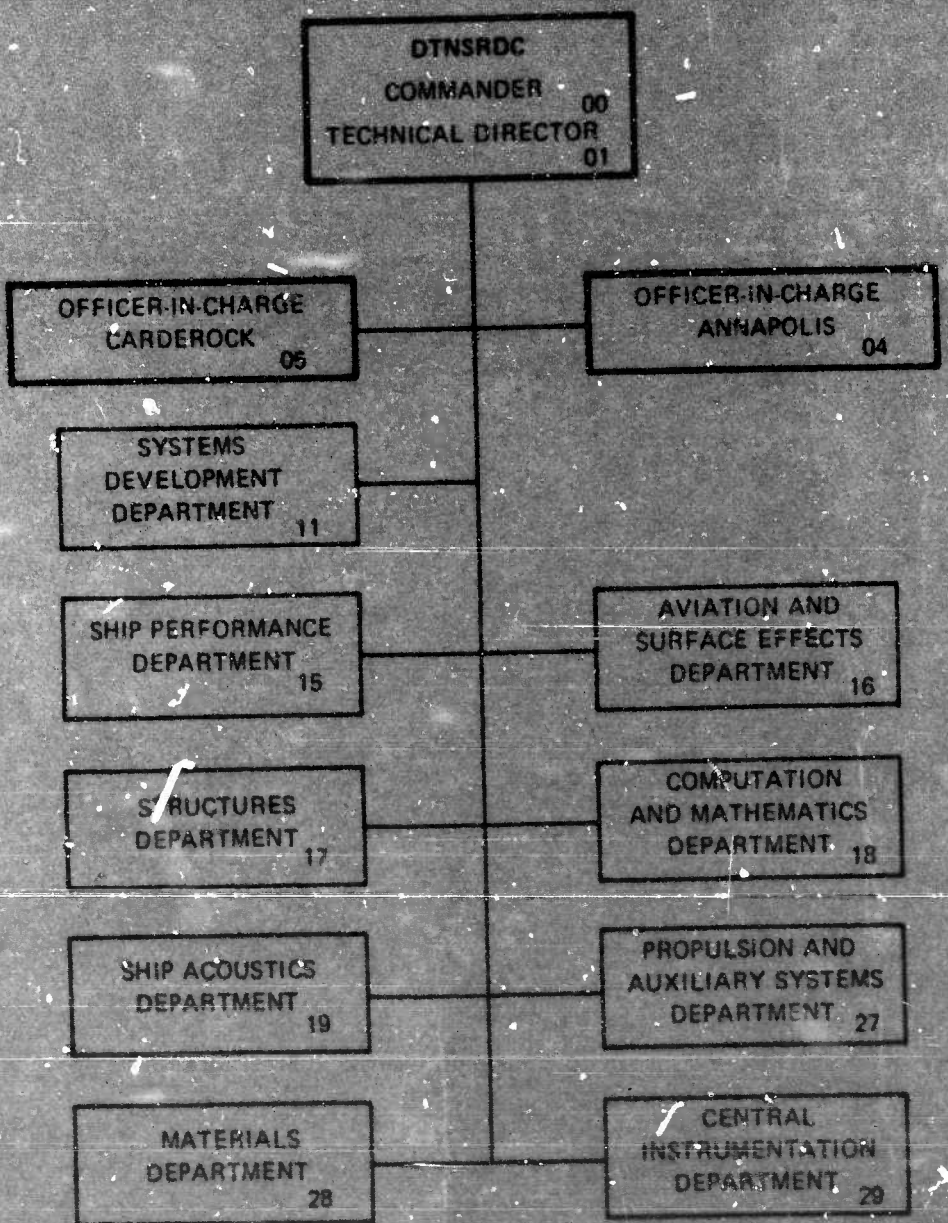

UNCLASSIFIED

SECURITY CLASSIFICATION OF THIS PAGE (When Data Entered)

REPORT DOCUMENTATION PAGE

READ INSTRUCTIONS BEFORE COMPLETING FORM

1. REPORT NUMBER: 76-0068
2. GOVT ACCESSION NO.:
3. RECIPIENT'S CATALOG NUMBER:

4. TITLE (and Subtitle): THEORETICAL DETERMINATION OF PORPOISING INSTABILITY OF HIGH-SPEED PLANING BOATS
5. TYPE OF REPORT & PERIOD COVERED:
6. PERFORMING ORG. REPORT NUMBER: DTNSRDC - 76-0068

7. AUTHOR(s): Milton Martin
8. CONTRACT OR GRANT NUMBER(s): SR023-01-01

9. PERFORMING ORGANIZATION NAME AND ADDRESS: David W. Taylor Naval Ship Research and Development Center, Bethesda, Maryland 20084
10. PROGRAM ELEMENT, PROJECT, TASK AREA & WORK UNIT NUMBERS: SR023-0101 Work Unit 1-1562-002

11. CONTROLLING OFFICE NAME AND ADDRESS:
12. REPORT DATE: April 1976
13. NUMBER OF PAGES: 73

14. MONITORING AGENCY NAME & ADDRESS (if different from Controlling Office): Naval Sea Systems Command, Washington, D. C. 20362
15. SECURITY CLASS. (of this report): UNCLASSIFIED
15a. DECLASSIFICATION/DOWNGRADING SCHEDULE:

16. DISTRIBUTION STATEMENT (of this Report)

APPROVED FOR PUBLIC RELEASE: DISTRIBUTION UNLIMITED

17. DISTRIBUTION STATEMENT (of the abstract entered in Block 20, if different from Report)

18. SUPPLEMENTARY NOTES

19. KEY WORDS (Continue on reverse side if necessary and identify by block number)

Planing Craft
Stability
Porpoising
Seakeeping
Pleasure Craft
Nonmilitary Application

20. ABSTRACT (Continue on reverse side if necessary and identify by block number)

A theoretical method is derived for predicting trim angle and speed coefficient at the inception of porpoising of prismatic planing hulls. Although equations are derived for the surge, pitch, and heave degrees of freedom, it is seen that the effect of surge is small at ordinary operating trim angles. Comparisons of theoretical predictions with existing experimental data on coupled pitch and heave porpoising show reasonably good agreement for a wide range of speed coefficients, load coefficients, and deadrise angles. The theory

(Continued on reverse side)

DD FORM 1 JAN 73 1473 EDITION OF 1 NOV 65 IS OBSOLETE
S/N 0102-014-6601

UNCLASSIFIED

SECURITY CLASSIFICATION OF THIS PAGE (When Data Entered)

(Block 20 continued)

may also be used for estimating the natural frequencies and damping characteristics of prismatic hulls in the stable, high-speed planing range.

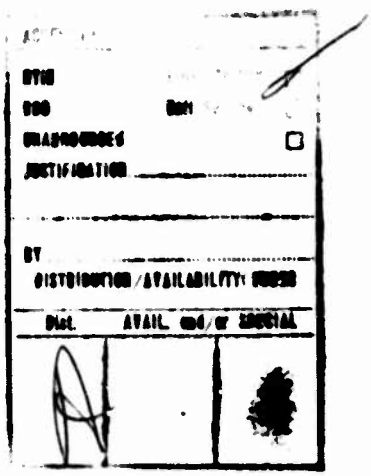

TABLE OF CONTENTS

LIST OF FIGURES

LIST OF TABLES

NOTATION

a	Value s at transverse plane through boat center of gravity
B	Bobyleff's function of deadrise; see Equation 54
b	Beam of boat
$C_{D,c}$	Cross flow drag coefficient; see Table 2
C_f	Hydrodynamic friction coefficient
C_{Lb}	Boat lift coefficient, nondimensionalized by the beam $2C_\Delta/C_V^2$
C_V	Speed coefficient, $U/\sqrt{gb}$
C_Δ	Load coefficient, $\Delta/\rho gb^3$
e_1, e_2	Coordinate measured parallel to keel from transom of tow point and resultant of wind force, respectively
F_{BS}	Steady state buoyancy force
F_D	Dynamic part of hydrodynamic normal force on hull
F_{DS}	Steady state part of F_D
F_{FS}	Steady state hull friction force
F_{WS}	Steady state wind drag
$f(k_n, e_n)$	Nondimensional moment arm about the center of gravity of tow force n = 1 and wind force n = 2
$f(\beta)$	Deadrise function of Wagner; see Equation 53
g	Acceleration of gravity
$g(k_n, e_n)$	Negative of derivative of $f(k_n, e_n)$ with respect to trim angle τ
$h(\tau)$	See Equation (96)
I_y	Pitch moment of inertia about the boat center of gravity
k_1, k_2	Coordinate measure normal to keel of tow point and resultant wind force, respectively
k_y	Radius of gyration of boat with respect to center of gravity
$\overline{LCG}$	Distance from transom to boat center of gravity, measured parallel to keel
l_g	Same as $\overline{LCG}$
l_k	Length of wetted portion of keel
M	Hydrodynamic pitch moment relative to center of gravity
M_{BS}	Steady state pitch moment due to buoyancy
M_D	Dynamic part of hydrodynamic pitch moment on hull
M_{DS}	Steady state part of M_D

M_{FS}	Steady state hull friction pitch moment
M_S	Total steady state pitch moment acting on hull
M_{TS}	Pitch moment about center of gravity due to towing force
M_{WS}	Pitch moment about center of gravity due to wind force
M_z, $M_{\dot{z}}$, M_θ, etc.	Partial derivative of pitch moment with respect to motion variables z, $\dot{z}$, θ, etc., respectively
m	Mass of boat
P	See Equation (78)
Q	See Equation (78)
s	Coordinate measured along keel from foremost immersed station of keel; see Figure 20
s_{c1}	See Equation (73) and Figure 20
s_{c2}	See Equations (76) and (77) and Figure 20
T_S	Steady state towing force
t	Time
U	Steady reference speed of boat in feet per second
u, $\dot{u}$	Perturbation surge velocity and acceleration
W	Boat weight
X	Hydrodynamic force component in direction of positive x
X_D	Dynamic part of hydrodynamic X-force
X_S	Steady state part of X
X_u, $X_{\dot{u}}$, $X_{\ddot{z}}$, etc.	Partial derivative of X-force with respect to motion variables u, $\dot{u}$, $\ddot{z}$, etc., respectively
x	Horizontal coordinate in direction of U
Z	Hydrodynamic force component in direction of positive z
Z_D	Dynamic part of hydrodynamic Z-force
Z_S	Steady state part of Z
Z_z, $Z_{\dot{z}}$, Z_θ, etc.	Partial derivative with respect to motion variables z, $\dot{z}$, θ, etc., respectively
z	Vertical coordinate, positive down
β	Deadrise angle; see Figure 20
Δ	Boat weight, W
ΔF_D	Time dependent part of F_D
ΔM_D	Time dependent part of M_D
ΔT_S	Time dependent part of towing force

ΔX_D	Time dependent part of X_D
ΔZ_D	Time dependent part of Z_D
$\zeta, \dot{\zeta}$	Components, normal to the keel, of hull velocity and acceleration, respectively
θ	Boat pitch angle perturbation, positive bow up
λ	Mean wetted length-to-beam ratio
λ_c	Length of wetted chine-to-beam ratio
λ_{c1}	Nondimensional value of s_{c1}, s_{c1}/b
λ_{c2}	Nondimensional value of s_{c2}, s_{c2}/b
λ_g	Nondimensional value $\overline{LCG}$, $\overline{LCG}/b$
λ_{gc}	Value of λ_g at inception of porpoising
λ_k	Nondimensional value of l_k, l_k/b
λ_{mc}	Value of λ at inception of porpoising
λ_v	Nondimensional value of normal distance of center of gravity from keel
μ	Total sectional added mass
μ_a	Contribution to sectional added mass
μ_s	Sectional added mass at transom
ν	Kinematic viscosity
ξ	Boat-damping ratio
ρ	Mass density of water
σ	Stability root; see Equation (22)
τ	Steady state trim angle measured from keel line to calm water free surface at reference speed U
τ_c	Value of τ at inception of porpoising
$\phi(\lambda)$	Three-dimensional or aspect ratio correction; see Figure 21
∇	Volume of water displaced at rest, cu ft

The prime (′) symbol is generally used to denote quantities in nondimensional form. Factors used for nondimensionalizing the previously described quantities are ρ, U, b. Typical examples are given as follows:

$$F_{BS}' = F_{BS}/(1/2\ \rho U^2 b^2) \qquad \lambda_{c1} = s_{c1}/b$$

$$M_{BS}' = M_{BS}/(1/2\ \rho U^2 b^3) \qquad \mu' = \mu/1/2\ \rho b^2$$

$$M_{\ddot{\theta}}' = M_{\ddot{\theta}}/(1/2\ \rho b^5) \qquad \sigma' = \sigma b/U$$

$$t' = tU/b$$

ABSTRACT

A theoretical method is derived for predicting trim angle and speed coefficient at the inception of porpoising of prismatic planing hulls. Although equations are derived for the surge, pitch, and heave degrees of freedom, it is seen that the effect of surge is small at ordinary operating trim angles. Comparisons of theoretical predictions with existing experimental data on coupled pitch and heave porpoising show reasonably good agreement for a wide range of speed coefficients, load coefficients, and deadrise angles. The theory may also be used for estimating the natural frequencies and damping characteristics of prismatic hulls in the stable, high-speed planing range.

ADMINISTRATIVE INFORMATION

This investigation was authorized and funded by the Naval Sea Systems Command (SEA 035) under the General Hydrodynamics Research Program, SR-023-0101, Work Unit 1-1562-002.

INTRODUCTION

Porpoising is an instability in pitch and heave experienced by planing craft traveling at high speeds on calm water. It has been known to lead to such violent motions as to cause many serious boating accidents. With constantly increasing boat speeds, this phenomenon is becoming more and more of a problem to planing- boat designers.

Perhaps the first attempt at treating this problem analytically was made by Perring,[1] who developed a theory for porpoising based on low-aspect-ratio wing theory. The practical application of this theory was unsuccessful since the theory was oversimplified. Since then, a great deal of experimental work has been done concerning porpoising for water-based aircraft and planing boats, and more recently additional attempts[2,3] at developing a theoretical treatment have met with varying degrees of success. Perhaps the only systematic experimental investigation for planing boats was done by Day and Haag[4] on prismatic bodies. These bodies comprised a wide range of design parameters. The results of this work have been widely used as

---

[1] Perring, W.G.A. and H. Glauert, "Stability on the Water of a Seaplane in the Planing Condition," Aeronautical Research Council, TR Vol. 42 (Sep 1933). A complete listing of references is given on pages 60 and 61.

[2] Lutowski, R.N., "A Computer Program for Various Performance Aspects of Planing Craft," Thesis submitted to Stevens Institute of Technology, Castle Point, Hoboken, N.J. (1973).

[3] Payne, P.R., "Coupled Pitch and Heave Porpoising Instability in Hydrodynamic Planing," Journal of Hydronautics, Vol. 8, No. 2 (Apr 1974).

[4] Day, J.P. and R.J. Haag, "Planing Boat Porpoising" Thesis Submitted to Webb Institute of Naval Architecture, Glen Cove, Long Island, N.Y. (May 1952).

a guide in estimating the porpoising limits of planing hulls.[5] Although this is a reasonable empirical approach, it does not contribute much to a good theoretical understanding of the problem. Such an understanding is required to determine the effects of variations in hull parameters of practical boats as well as to evaluate innovative ideas for prevention of porpoising. Furthermore, it is important for providing a tool for estimating the effects of design parameters on natural oscillation frequencies and damping characteristics of the boat, since these characteristics play a dominant role in dynamic behavior in a seaway. In fact, the theoretical approach derived herein has been used in development of a linearized theory for predicting the motions of planing boats of arbitrary deadrise angle in waves.[6]

Although the theory has been developed for prismatic planing hulls, it appears to be suitable as a guide for predicting effects of parameter variation on porpoising of practical planing-boat configurations. Furthermore, the methods used lend themselves to direct extension to a theory for nonprismatic hulls.

STABILITY EQUATIONS

Stability equations for the longitudinal motions in surge, pitch, and heave are derived in Appendix A. To make comparisons with the large quantity of existing porpoising data from towed models, provision was made to include the effect of the tow force. Since the models were towed at constant speed, the surge equation played no role in determination of the boat model stability; only the coupled pitch and heave equations were needed to investigate the problem. However, it is believed that the results obtained in this manner are generally applicable to boats with all three degrees of freedom, since, as shown in Appendix A, the magnitude of the stability derivatives in the surge equation are considerably smaller than those in the pitch and heave equations for most cases of interest. We therefore used the following nondimensional* linearized stability equations for the dynamic heave force and pitch moment equilibrium, respectively.**

[5] Savitsky, D., "Hydrodynamic Design of Planing Hulls," Marine Technology (Oct 1964).

[6] Martin, M., "Theoretical Determination of Motion of High-Speed Planing Craft in Waves," DTNSRDC Report 76-0069 (Apr 1976).

*The prime symbol, normally used to denote a nondimensional quality, is omitted for convenience.

**The effect of the surge degree of freedom is readily determined from the stability equations for surge, pitch, and heave as derived in Appendix A.

$$(Z_{\ddot{z}} - m)\ddot{z} + Z_{\dot{z}}\dot{z} + Z_z z + Z_{\ddot{\theta}}\ddot{\theta} + Z_{\dot{\theta}}\dot{\theta} + Z_\theta \theta = 0 \tag{1}$$

$$M_{\ddot{z}}\ddot{z} + M_{\dot{z}}\dot{z} + M_z z + (M_{\ddot{\theta}} - I_y)\ddot{\theta} + M_{\dot{\theta}}\dot{\theta} + M_\theta \theta = 0 \tag{2}$$

These equations describe the motion relative to fixed horizontal and vertical axes, 0 x and 0 z, along and at right angles to the direction of motion; see Figure 1. The origin 0 was taken at the boat center of gravity and moves with the constant reference speed U of the boat. The symbols Z and z represent the vertical force and displacement, respectively, at 0, positive in the down direction. The symbols M and θ are the pitch moment and angular displacement perturbation, respectively, with respect to the origin 0, positive in the sense of bow up. The coefficients of the variables $\ddot{z}$, $\dot{z}$, z, $\ddot{\theta}$, $\dot{\theta}$, and θ are the stability derivatives; e.g., $Z_{\ddot{\theta}}$ is the nondimensional linearized rate of increase of vertical force Z with nondimensional angular acceleration $\ddot{\theta}$.

The stability derivatives have been derived for constant deadrise planing hulls in Appendix A in terms of the geometric and operational characteristics of the boat. They were derived on the assumption that the craft could be treated as a slender body with an empirical three-dimensional correction. Because of the high Froude number range of operation and the low aspect ratio, wavemaking and unsteady lift effects were assumed negligible.

The velocity and acceleration derivatives (Appendix A) are

$$Z_{\ddot{z}} = -\varphi(\lambda)\cos^2\tau \int \mu'\, ds' \tag{3}$$

$$Z_{\dot{z}} = -2\,\varphi(\lambda)\,\mu_s'\cos^3\tau \tag{4}$$

$$Z_{\ddot{\theta}} = \varphi(\lambda)\int \mu'(a' - s')\, ds' \tag{5}$$

$$Z_{\dot{\theta}} = -2\,\varphi(\lambda)\,\mu_s'\,\lambda_g\cos^2\tau \tag{6}$$

$$M_{\ddot{z}} = \varphi(\lambda)\cos\tau \int \mu'(a' - s')^2\, ds' \tag{7}$$

$$M_{\dot{z}} = 2\,\varphi(\lambda)\cos^2\tau\left(\int \mu'\, ds' - \lambda_g\,\mu_s'\right) \tag{8}$$

$$M_{\ddot{\theta}} = -\varphi(\lambda)\int \mu'(a' - s')^2\, ds' \tag{9}$$

$$M_{\dot{\theta}} = -2\,\varphi(\lambda)\cos\tau\left(\mu_s'\,\lambda_g^2 + \int \mu'(a' - s')\, ds'\right) \tag{10}$$

where τ = equilibrium trim angle

λ = mean wetted length-to-beam ratio

$\phi(\lambda)$ = three-dimensional correction factor

μ' = nondimensional sectional added mass

μ_s' = nondimensional sectional added mass at transom

λ_g = nondimensional distance from transom to center of gravity

s' = nondimensional distance from foremost wetted point on keel to any boat section; see Figure 20

a' = value of s' at boat center of gravity

The integrations have been taken over the wetted length of the boat. Expressions for the sectional added mass distribution are derived in Appendix A.

The so-called static derivatives are obtained directly from the expressions for the steady state Z_S' force and M_S' moment. Since both are functions of λ and τ, and $\lambda = \lambda(z, \tau)$, we have

$$Z_z = \frac{\partial Z_S'}{\partial \lambda} \frac{\partial \lambda}{\partial z'} \tag{11}$$

$$Z_\theta = \frac{\partial Z_S'}{\partial \tau} + \frac{\partial Z_S'}{\partial \lambda} \frac{\partial \lambda}{\partial \tau} \tag{12}$$

$$M_z = \frac{\partial M_S'}{\partial \lambda} \frac{\partial \lambda}{\partial z'} \tag{13}$$

$$M_\theta = \frac{\partial M_S'}{\partial \tau} + \frac{\partial M_S'}{\partial \lambda} \frac{\partial \lambda}{\partial \tau} \tag{14}$$

The steady state Z_S' force which is the negative of the lift force (Appendix A) is

$$Z_S' = -\varphi(\lambda)\,\mu_s' \sin\tau \cos^2\tau + \frac{0.624}{C_V{}^2}\lambda^2 \sin\tau\cos\tau - \lambda\, C_f \sin\tau/\cos\beta \tag{15}$$

where

β = deadrise angle

$C_V = U/\sqrt{gb}$ = speed coefficient

C_f = skin friction coefficient

The first term is the dynamic lift on the hull; the second term is the hydrostatic lift, and the last term is the vertical component of the skin friction force, assumed to act parallel to the keel line.

The expression for the steady state moment M_S' about the boat center of gravity (Appendix A) is

$$M_S' = \varphi(\lambda)\sin\tau\cos\tau\left(\int \mu'\, ds' - \mu_s'\lambda_g\right) + \frac{0.624\sin\tau}{C_V{}^2}\lambda^2\left(\frac{\lambda}{3} - \lambda_g\right)$$

$$- \frac{C_f}{\cos\beta}\lambda\left(\lambda_v - \frac{\tan\beta}{4}\right) - T_S' f(k_1, e_1) + F_{WS}' f(k_2, e_2) \tag{16}$$

where

T_S' = nondimensional towing force = drag

F_{WS}' = nondimensional aerodynamic drag

$f(k_1, e_1)$ = moment arm of towing force

$f(k_2, e_2)$ = moment arm of aerodynamic force

The equation for T_S' (Equation (90) of Appendix A) is

$$T_S' = -Z_S' \tan \tau + \frac{\lambda C_f}{\cos \beta \cos \tau} + F_{WS}' \tag{17}$$

The first term in Equation (16) is the hydrodynamic moment, the second term is the hydrostatic moment and the third term is the moment due to skin friction. The last two terms are the moment due to the tow force and the aerodynamic drag.

The steady state values of λ and τ used in Equations (3) through (14) are determined from the following equations of planing equilibrium.

$$W' + Z_S' = 0 \tag{18}$$

$$M_S' = 0 \tag{19}$$

These equations are solved by an iteration process described in Appendix A.

The solution to Equations (1) and (2) are

$$z' = z_1 e^{\sigma_1' t'} + z_2 e^{\sigma_2' t'} + \ldots\ldots \tag{20}$$

$$\theta = \theta_1 e^{\sigma_1' t'} + \theta_2 e^{\sigma_2' t'} + \ldots\ldots \tag{21}$$

where $z_1, z_2, \cdots \theta_1, \theta_2, \cdots$ are constants which depend on the initial conditions. The σ' terms determine the character of the time history response of the boat to any small disturbance. Four values of σ' are obtained from the roots of the resulting characteristic equation.

$$A\sigma'^4 + B\sigma'^3 + C\sigma'^2 + D\sigma' + E = 0 \tag{22}$$

where

$$\begin{aligned} A &= (Z_{\ddot{z}} - m)(M_{\ddot{\theta}} - I_y) - M_{\ddot{z}} Z_{\ddot{\theta}} \\ B &= Z_{\ddot{z}}(M_{\dot{\theta}} - I_y) + (Z_{\dot{z}} - m) M_{\dot{\theta}} - M_{\ddot{z}} Z_{\dot{\theta}} - M_{\dot{z}} Z_{\ddot{\theta}} \\ C &= Z_z(M_{\ddot{\theta}} - I_y) + Z_{\dot{z}} M_{\dot{\theta}} + (Z_{\ddot{z}} - m) M_\theta - M_{\ddot{z}} Z_\theta - M_{\dot{z}} Z_{\dot{\theta}} - M_z Z_{\ddot{\theta}} \\ D &= Z_z M_{\dot{\theta}} + Z_{\dot{z}} M_\theta - M_{\dot{z}} Z_\theta - M_z Z_{\dot{\theta}} \\ E &= Z_z M_\theta - M_z Z_\theta \end{aligned} \tag{23}$$

The roots of these equations may be real or complex conjugate pairs. In either case, it is seen from Equations (20) and (21) that if any root has a positive real part, the transient response increases without limit, and the boat is considered unstable in the linear sense.

In general, a complex pair of roots represents an oscillatory mode, e.g., for the root pair $\sigma' = \sigma_R' \pm i\sigma_I'$, the z' response is

$$z' = e^{\sigma_R' t'} (C_1 \cos \sigma_I' t' + C_2 \sin \sigma_I' t')$$

where C_1 and C_2 are real constants which are determined by the initial conditions. The magnitude of the imaginary part of the root σ_I' is the nondimensional natural frequency of the modal motion. In dimensional form the natural frequency and period are

$$\sigma_I = \sigma_I' \frac{U}{b} \text{ rad/sec} \tag{24}$$

$$T = \frac{2\pi}{\sigma_I} \text{ sec} \tag{25}$$

The effect of the real part of the root σ_R' may be illustrated by computing the time for a disturbance to either halve or double itself in magnitude. Thus, if σ_R' is negative, the envelope of the disturbance will be halved when

$$e^{\sigma_R' t'} = e^{\sigma_R t} = 1/2$$

It follows that the time for the disturbance motion of each mode to halve or double itself is

$$t_{1/2} \text{ or } t_2 = 0.69/\sigma_R \text{ sec} \tag{26}$$

Another useful measure of damping of oscillatory modes is the damping ratio ξ, which is directly related to the rate of decay of disturbance oscillations.

It is given by

$$\xi = -\frac{\sigma_R}{\sqrt{\sigma_R^2 + \sigma_I^2}} \tag{27}$$

In the vicinity of the resonant encounter frequency in waves, the damping ratio is also inversely related to the amplification ratio of the boat response. Values of ξ between 0.6 and 1.0 are usually considered to give well-damped modes. Values less than about 0.4 are generally considered to produce underdamped modes. Although the forgoing may provide a rough indication of the vertical plane dynamic characteristics of the boat, a dynamic motions analysis is required for any detailed study.

DETERMINATION OF PORPOISING CONDITIONS

Perhaps the only systematic experimental investigation of porpoising was carried out in 1952 by Day and Haag.[4] Measurement by other investigators[7,8,9] have generally been incidental to a broader program primarily concerned with resistance. The experiments of Day and Haag were carried out with 3.8-inch-beam, prismatic wood models towed by a light line from a point slightly forward of and above the center of gravity. Deadrise angles of 0, 10.6, and 20.5 degrees were investigated. The load coefficients were 0.36, 0.48, and 0.72. For each speed the boat center of gravity was gradually moved aft until the boat porpoised. The trim at which this occurred defined the critical trim angle and provided a point on the trim angle versus speed stability boundary. Values of the mass and moment of inertia for practically all the models at porpoising were provided. Thus, it was possible to make a theoretical calculation for each test condition. Small allowances for aerodynamic effects and chine corner radius were made. These are described in Appendix B.

Calculations of each of the four stability roots for each test condition were obtained from Equation (22). In the vicinity of porpoising, the least stable root was complex in each case, indicating that the response to a disturbance would always be oscillatory. Figure 2 is a typical plot of the variation of the real part of the least stable root σ_{R1}' with the nondimensional longitudinal distance λ_g of the center of gravity from the transom for three of the test speeds with β = 10.6 degrees and C_Δ = 0.48. It is seen that the stability roots become negative (stable) for values of λ_g less than about 0.20 and greater than about 0.85 for the cases shown. We note that in the stable region, corresponding to the small λ_g range, the equilibrium trim angles are much higher than in the stable region of the high λ_g range. Also, the magnitude of the stability root in the small λ_g range is usually quite small, so that the damping of the boat oscillations may usually be expected to be poor. Taking an example from the figure, we find from Equation (26) that the time for a disturbance to damp to half amplitude at C_V = 2.67 would be more than 15 seconds for a boat with a 15-foot beam, and σ_{R1}' = -0.01. This would be intolerable in the presence of even very small disturbances. On the other hand, it is seen from the same figure that moving the center of gravity forward of the upper value at which the root becomes negative results in increasingly negative values of the stability root and,

---

[7] Fridsma, G., "A Systematic Study of Rough-Water Performance of Planing Boats," Davidson Laboratory, Stevens Institute of Technology, Hoboken, N.J., Report 1275 (Nov 1969).

[8] Clement, E.P. and D. Blount, "Resistance Tests of Systematic Series of Planing Hull Forms," Transactions Society of Naval Architects and Marine Engineers, Vol. 71, pp. 491 - 561 (1963).

[9] Davidson, K.S.M. and A. Suarez, "Tests of Twenty Related Models of V-Bottom Motor Boats - EMB Series 50," David Taylor Model Basin Report R-47 (1949).

therefore, considerably higher damping for this mode. For example, for the same speed and $\lambda_g = 1.5$, we find $\sigma_{R1}' = 0.3$, and the time for a disturbance to damp to half amplitude is of the order of only one-half second. Since the calculated value of σ_{I1}' at this condition is about 0.5, the damping ratio from Equation (27) is found to be approximately 0.50; whereas, for the previous condition it was only about 0.02.

An alternative plot to Figure 2 showing the variation of the calculated σ_{R1}' with trim angle, for a complete range of test speeds, with $\beta = 0$ degrees and $C_\Delta = 0.72$, is shown in Figure 3. This plot is typical of those used to determine the critical trim angle as a function of the speed coefficient. Where two trim angles at zero root crossing are shown, the smaller trim angles are taken. The porpoising boundaries thus determined are discussed in the next section.

COMPARISONS WITH EXPERIMENTS ON PRISMATIC HULLS

Figure 4 shows the variation, with the speed coefficient C_V, of the critical trim angle of a prismatic planing configuration, with a deadrise angle of zero degrees, for three values of load coefficient. The points in the figure represent the experimental data.[4] The curves were obtained from the present theory. It is seen that the theory agrees reasonably well with the experiments for $C_\Delta = 0.36$ and 0.72. For the intermediate load coefficient $C_\Delta = 0.48$, the theory gives intermediate values of critical trim angle; whereas, the data for this condition are close to those obtained at $C_\Delta = 0.36$.

Figure 5 is a similar set of graphs for the prismatic hull with a deadrise angle of 10.6 degrees. Here, the agreement between the theory and the experimental results over the whole speed range is quite good for $C_\Delta = 0.48$ and 0.72. However, for $C_\Delta = 0.36$, the theory tends to underpredict the critical trim angle about 1 degree at the higher speeds. Part of this discrepancy is due to the fact that the chine became unwetted at the transom, and the theory does not account for this.* The discrepancy tends to be greatest at the highest speeds and for the lowest loading conditions. The region where the whole chine is out of the water is indicated approximately by the dashed portion of the curve.

Figure 6 is a similar comparison for a hull with deadrise angle of 20.5 degrees. Here the theoretical curve tends to fall slightly lower than the data, at the lower speeds, and underpredicts the critical trim angle by about one degree at the higher speeds. In this case the chine became unwetted sooner than for the boat with a 10.6 degree deadrise angle. The approximate region of occurrence is indicated by the dashed portion of the curves. An attempt was

*The theory is being modified to include these effects.

made to determine the effect of modifying the magnitude of the lower limit of integration in part of the added mass integral as discussed in Appendix A. This had the effect of further improving the predictions as shown by the broken curves in Figure 6. This slight alteration to the theory had practically no effect on the predicted porpoising boundaries for the hulls having 0- and 10.6-degree deadrise angles.

Day and Haag found that by plotting the measured trim angle against $(C_{Lb}/2)^{1/2}$ or $\sqrt{C_\Delta}/C_V$, the separate curves for each load coefficient collapsed into a narrow band. This result was also found from the theoretical calculations. Figures 7 through 9 show comparisons between the experimental data and the calculations plotted in this manner. Except as noted earlier, it is seen that the overall agreement between the theory and the data is reasonably good for all of the deadrise conditions investigated.

For each critical trim angle τ_c, the corresponding critical position of the boat center of gravity λ_{gc}, must satisfy the steady state equilibrium equations. Thus the degree of agreement between the measured and predicted magnitude of λ_{gc} is, in part at least, a measure of the accuracy of the steady state equations. Figure 10 shows a comparison with theory of the measured variation of λ_{gc} with speed coefficient for each of the conditions investigated by Day and Haag. It is seen that the best overall agreement was obtained for the hull with zero deadrise angle. For the deadrise angles of 10.6 and 20.5 degrees, the calculations were about 10 to 15 percent lower than the measurements.

This result seems to be consistent with the tendency of the steady state Equations (18) and (19) to underestimate the steady trim angle, thus requiring a more aft position of the center of gravity to obtain a given trim angle. Comparison with the steady state trim data in Reference 7 of a similar formulation recently proposed by Brown[10] exhibits the same tendency to approximately the same degree. However, the empirical formulation presented by Savitsky[5] does not show this tendency and gives, on the average, better agreement with measured steady state trim angles. As will be seen later, the use of this formulation generally gives larger values of λ_g for a given value of τ.*

Another interesting feature of Figure 10 is that the effect of load coefficient appears to be small. This is mainly due to the fact that the more highly loaded configurations of the Day and Haag models had smaller radii of gyration. As will be seen later, the theory shows that these two effects are generally compensatory in their effect on the critical center of gravity position. It is also worth mentioning that the theoretical values of the location of the

[10] Brown, P.W., "An Experimental and Theoretical Study of Planing Surfaces with Trim Flaps," Davidson Laboratory, Stevens Institute of Technology, Hoboken, N.J., Report 1463 (Apr 1971).

*The reasons for this discrepancy are being investigated.

hydrodynamic center of pressure and center of gravity were within 5 percent of each other in nearly all cases. As one might expect, this was the case throughout the stable operating range as well.

Figure 11 is a plot of the theoretical nondimensional mean wetted length of the boat at porpoising against speed coefficient for the various conditions investigated. Unfortunately, Day and Haag did not measure the wetted length of their models, so no direct comparison with the data is possible. Average values of observed wetted lengths of the spray sheet at the chine, which did not vary much with speed, are shown for a rough comparison. As one might expect the spray sheet length relative to the mean wetted length becomes smaller with increasing deadrise angle.[5]

For a typical configuration, Figures 12 and 13 show the separate effect of nondimensional loading C_Δ and radius of gyration k_y/b on the magnitude of the critical trim angle τ_c as determined from the theory. It is seen that τ_c becomes smaller with both increasing radius of gyration and load coefficient. However, the effect is not large -- especially for small values of C_{Lb}.* It will be recalled that the higher the loading the smaller was the radius of gyration for the models investigated by Day and Haag. This effect also contributed, to some extent, to collapse of their data for different load conditions. A similar effect, though more pronounced, may be shown to hold with respect to the critical nondimensional value of the longitudinal center of gravity position and mean wetted length. Figures 14 through 16 show that the value of λ_{gc} and λ_{mc} increases with both increasing C_Δ and increasing k_y/b. Here these effects account almost entirely for the tendency of the λ_{gc} versus C_V curves (Figure 10) and the λ_{mc} versus C_V curves (Figure 11) to collapse into a narrow band for the various loadings shown.

Although, the calculated values of λ_{gc} tend to be low, Figures 14 and 15 nevertheless illustrate some interesting trends. It is seen that the value of λ_{gc} has an increasing tendency to reach a limit with increasing deadrise angle and decreasing load coefficient. Also the value of λ_{gc} becomes smaller with decreasing nondimensional radius of gyration and increasing deadrise angle. It thus appears that high deadrise angle, low loading, and a small radius of gyration permit a more aft location of the critical center of gravity. Furthermore, it appears that the tendency for the curve to turn down at the higher deadrise angles may explain the observation by Stolz[8] and others that "deadrise surfaces which are not deep into the porpoising range often regain stability at higher speeds."

Relatively recently Fridsma[7] reported a rather limited amount of experimental data on the porpoising of prismatic hulls with deadrise angles of 10, 20, and 30 degrees and with

*Theory and experiment show, however, that natural frequency of oscillatory motion decreases significantly with increasing moment of inertia.

various load coefficients. Experiments for the 20 degree deadrise case were carried out with models of length-to-beam ratio of 4, 5, and 6 so that different values of k_y/b were obtained for the same C_Δ in some cases. Figures (17a) and (17b) show a comparison of measured values of critical trim angle made by Fridsma with those computed from the theory. The theoretical curves are basically cross plots of curves such as those in Figure 12 for various load coefficients. They provide a convenient method of indicating the effect of variations in k_y/b, separately from C_{Lb} and C_Δ on the magnitude of τ_c. It may be seen from the figure that the theory predicts τ_c quite well in most cases but that there are insufficient data to verify the variation with k_y/b predicted by the theory.

The calculated values of λ_{gc} and λ_{mc} in these cases were about 28 and 15 percent lower, respectively, than the measured values. The former is more than twice the difference computed for the Day and Haag experiments. As noted earlier, this was felt to be due mainly to the fact that the steady state equations tend to underpredict steady state trim angle. Values of λ_{gc} were then recalculated for each of the theoretical values of τ_c from the following steady state equations, adapted from Reference 5.

$$\lambda_p = 0.75\,\lambda - \frac{\lambda}{(5.21\,C_V^2/\lambda^2) + 2.39} \approx \lambda_g \tag{28}$$

where λ_{mc} is defined by the following equations

$$C_{Lo} = \tau_c^{1.1}(0.0120\,\lambda_{mc}^{1/2} + 0.0055\,\lambda_{mc}^{5/2}/C_V^2)$$

$$C_{Lb} = C_{Lo} - 0.0065\,\beta\,C_{Lo}^{0.60}$$

and λ_p is the nondimensional distance of the center of pressure forward of the transom. The assumption that the center of pressure and center of gravity are coincident was found from the theory to be valid to within a few percent in nearly all cases. The use of the above equations resulted in better agreement with the experimental values when the theoretical values of τ_c were substituted. Table 1 shows a comparison of λ_{gc} thus obtained with the measured values. Also shown are comparisons with the measured mean wetted lengths. It is seen that the calculated values are within a few percent of the measurements in nearly all cases.

COMPARISONS WITH EXPERIMENTS ON NONPRISMATIC HULLS

Although the theory and data presented thus far are for prismatic hull forms, they show trends which are close to those observed on a variety of nonprismatic models. Two principle sets of data[8,9] are available for comparison. The DTMB Series 62 models of Clement and Blount[8] are pure monohedran hulls with a transom-to-beam ratio between 0.64 and 0.80 and constant aft deadrise angle of 12.5 degrees. Those of Davidson and Suarez[9] have a low chine

TABLE 1 – COMPARISON BETWEEN CALCULATED AND MEASURED VALUES OF λ_{gc} AND λ_{mc}, USING COMPUTED CRITICAL TRIM ANGLE AND METHOD OF REFERENCE 5 FOR MEASURED PORPOISING CONDITIONS OF REFERENCE 7

Deadrise β deg	Load Coefficient C_Δ	Speed Coefficient C_V	$\frac{\lambda_{gc}\ \text{Calculated}}{\lambda_{gc}\ \text{Measured}}$	$\frac{\lambda_{mc}\ \text{Calculated}}{\lambda_{mc}\ \text{Measured}}$
10	0.912	3.83	0.86	0.94
	0.608	3.00	0.90	0.99
	0.304	3.33	0.93	1.06
	0.304	2.00	0.94	1.00
20	0.608	3.89	1.07	1.17
	0.608	2.73	1.03	0.97
	0.304	2.66	1.00	1.12
	0.304	2.98	1.02	1.00
30	0.609	2.73	1.02	0.95
	0.912	3.85	1.07	1.00

line and warped bottom with a transom-to-beam ratio of 0.88 and a mean deadrise angle between 4.0 and 7.3 degrees. In view of the approximate nature of the comparison it was felt that existing calculations for the 10.6-degree deadrise configurations would give a sufficiently good representation of the trends measured in the previously mentioned data.

The porpoising boundary described by Clement and Blount was presented as a plot of C_{Lb}/λ_{gc} versus the volumetric Froude number F_∇ where

$$C_{Lb} = 2\,C_\Delta/C_V{}^2$$

$$F_\nabla = U/\sqrt{\nabla^{1/3}} = C_V/(C_\Delta)^{1/6}$$

It is seen that the critical trim angle does not appear anywhere, and the porpoising boundary is expressed mainly in terms of the critical position of the center of gravity. This method of plotting was an apparent attempt to collapse the measured values of λ_{gc} for the wide range of load coefficients investigated. Figure 18 shows a comparison of the theoretical calculations with the Series 62 data. The theoretical curves are constructed from the calculated curves of Figure 10 for β = 10.6 degrees and C_Δ = 0.36, 0.48, and 0.72. The C_Δ values are in the approximate range of most of the data. The values of C_{Lb}/λ_{gc} given in Reference 8 were nondimensionalized with respect to the beam at the center of gravity, while those shown in Figure 18 have been based on the mean of the maximum beam and the beam at the transom in order to provide a more realistic comparison with the constant beam case. It is seen that the theoretical curve follows the same trend as the data but is about 10 to 15 percent higher.

This is mainly a reflection of the difference between predicted and measured values of λ_{gc} shown in Figure 10. It may be seen that the points for different loading conditions will fall on separate lines and that the trend with loading for each model is close to that given by the theory; e.g., compare Conditions 3, 4, and 5 with the trends shown in Figure 15.

It is easy to show that the measured effect of radius of gyration exhibits the same trends as that shown by the theory; see Figure 14. Although the radius of gyration k_y/b of the models was not measured, it is reasonable to assume that it was increasingly larger for the models with larger length-to-mean-beam ratio L_P/B_{PA}. By comparing the trends of the data for different models with approximately the same load coefficient (Conditions 1 with 3 and 5 with 6) we see that the value of λ_{gc} follows the trends with k_y/b predicted by the theory.

Clement and Blount found that the slope of a straight line through the data points was about -2.5. This implies that, for a given value of C_Δ

$$\lambda_{gc} \sim \sqrt{C_V}$$

since $C_{Lb} = 2\, C_\Delta/C_V{}^2$. From Figure 10 it is seen that the previously described equation would fit the theory and experimental data for the prismatic hulls quite well. Although the equation may be a good approximation for the data shown, it is seen from the theoretical curves of Figures 14 and 15 for k_y/b constant that it is not safe to assume that this is true in all cases.

The data of Davidson and Suarez[9] are most conveniently compared in the form of a porpoising boundary presented by Agnelli.[11] This is shown in Figure 19 as a plot of measured values of the critical trim angle τ_c against $2/(C_{Lb}/\lambda_{gc})$. Included also are the data points for the Series 62 hulls. These were recently obtained by the author from Mr. Blount and are not quite the same as those shown in the plot of Reference 11. Shown for comparison with the trends predicted by theory are straight lines drawn through points obtained from the calculated curves of Figures 5 and 10 for the case of β = 10.6 degrees and C_Δ = 0.36, 0.48, and 0.72. Although many of the points do not fall on the lines, it is clear that the trends are predicted. More detailed comparisons with the individual models must await further extension of the theory to include more general-type hull configurations.

CONCLUSIONS

A theoretical method has been derived for predicting the conditions leading to porpoising in the surge, pitch, and heave degrees of freedom of prismatic hulls with arbitrary deadrise angle. Comparisons of the theory with the porpoising boundaries measured on towed models

[11] Agnelli, J.C., "Evaluation of the Trim of a Planing Boat at Inception of Porpoising," presented at Spring Meeting of Society of Naval Architects and Marine Engineers, Lake Buena Vista, Fla. (Apr 1973).

with freedom only in pitch and heave showed reasonably good agreement. Since no porpoising data with all three degrees of freedom are available, it was not possible to check the theory for this case. However, from a comparison of the relative magnitudes of the coefficients in the surge equation it appears that this effect is small. In any case this may readily be investigated in more detail with the three degree of freedom stability equations in Appendix A.

The stability roots obtained from the characteristic equation provide estimates of the dynamic behaviour, such as oscillation natural frequencies and damping characteristics of the boat in the stable region.

Although the theory was developed for prismatic hull forms, it appears to be suitable as a guide in estimating the porpoising limits and dynamic characteristics of more conventional-type planing hulls, as well as the effects of variations in several of the parameters. It is felt that by an extension of the analytical methods used in the present analysis even closer agreement with data on prismatic hulls and conventional boats could be achieved, and a tool suitable for investigating the effects of detailed design modifications could be obtained.

ACKNOWLEDGMENTS

I wish to express my deep gratitude to Mr. Jacques B. Hadler, under whose supervision the present work was started, and to Mr. Grant R. Hagen, Head Ship Dynamics Division, for their continuing encouragement and interest in the present effort. My appreciation is also extended to Dr. William E. Cummins, Head Ship Performance Department and to Mr. Vincent J. Monacella for their valuable assistance and support. Furthermore, special thanks are due to Ms. Nadine Hubble, who developed the computer program and carried out all of the calculations with her characteristic skill and efficiency.

APPENDIX A

DERIVATION OF PORPOISING STABILITY EQUATIONS

It is assumed that the planing craft has a prismatic hull of constant deadrise, is moving at constant speed parallel to a calm water surface, and is free to perform small perturbation motions in pitch, heave, and surge about its steady equilibrium attitude. Since the theory is concerned mainly with the high-speed, low-aspect ratio condition, it is assumed that the craft may be treated as a slender body with an empirical three-dimensional correction, and unsteady effects are small. The kind of analysis to be used was first used in 1924 by Munk[12] and later by Jones[13] in connection with the analysis of airships and slender wings, respectively. More recently this method has been generalized by Bryson[14] for completely submerged slender-finned missiles. It has also been applied to the problem of pure translational impact of seaplanes on a calm water surface by Mayo[15] and others.[16,17]

FORCES DUE TO PERTURBATIONS IN VELOCITY AND ACCELERATION

The flow over the hull is assumed to occur in transverse planes which are fixed in space and oriented normal to the keel; see Figure 20. The momentum of each layer of water transverse to the keel is $\mu\dot{\zeta}ds$, where μ is the two-dimensional added mass of the section of the hull at point s, interacting with the section of the flow plane of length ds, and $\dot{\zeta}$ is the component of the velocity of the body normal to the keel at that point. The coordinate s is measured from the foremost immersed station along the keel. The normal force on the section ds of the hull is the time rate of change of the momentum of the layer of water ds at s.

---

[12] Munk, M.M., "The Aerodynamic Forces on Airship Hulls," National Advisory Committee for Aeronautics Report 184 (1924).

[13] Jones, R.T., "Properties of Low-Aspect-Ratio Wings at Speeds Below and Above the Speeds of Sound," National Advisory Committee for Aeronautics Report 835 (1946).

[14] Bryson, A.E., Jr., "Stability Derivatives for a Slender Missile with Application to a Wing-Body Vertical Tail Configuration," Journal of Aeronautical Sciences, Vol. 2 No. 5, pp. 297 - 308 (1955).

[15] Mayo, W.L., "Analysis and Modification of Theory for Impact of Seaplanes on Water," National Advisory Committee for Aeronautics Report 810 (1945).

[16] Milwitzky, B., "A Generalized Theoretical and Experimental Investigation of the Motions and Hydrodynamic Loads Experienced by V-Bottom Seaplanes During Step-Landing Impacts," National Advisory Committee for Aeronautics TN 1516 (1948).

[17] Schnitzer, E., "Theory and Procedure for Determining Loads and Motions in Chine-Immersed Hydrodynamic Impacts of Prismatic Bodies," National Advisory Committee for Aeronautics Report 1152 (1953).

$$dF_D = \frac{d}{dt}(\mu\dot{\zeta})\,ds \tag{29}$$

Both μ and $\dot{\zeta}$ will in general be functions of the longitudinal position coordinate x and time t. The time derivative is therefore

$$\frac{d}{dt} = -U\frac{\partial}{\partial x} + \frac{\partial}{\partial t} \tag{30}$$

where U is the steady state speed.

The normal hydrodynamic force over the entire hull is obtained by integrating Equation (29) along the wetted length of the hull l_k and multiplying by a correction factor $\phi(\lambda)$ to account for the three-dimensionality of the flow.

$$F_D = \phi(\lambda)\int_o^{\ell_k} \frac{d}{dt}(\mu\dot{\zeta})\,ds \tag{31}$$

where λ is the mean wetted length divided by the beam. A plot of $\phi(\lambda)$ obtained empirically by Pabst[18] is shown on Figure 21. The integral may be expressed as the sum of a velocity term and an acceleration term.

$$F_D = \varphi(\lambda)\left[\int_o^{\ell_k} \dot{\zeta}\frac{d\mu}{dt}ds + \int_o^{\ell_k} \mu\frac{d\dot{\zeta}}{dt}ds\right] \tag{32}$$

The longitudinal and heave perturbation velocities and accelerations are, respectively, denoted by u, $\dot{u}$, $\dot{z}$, $\ddot{z}$. The pitch angle perturbations are $\dot{\theta}$, $\ddot{\theta}$. From Figures 1 and 20 we obtain the following relationships:

$$\frac{ds}{dx} = -\cos\tau \tag{33}$$

$$\frac{\partial\zeta}{\partial x} = -\sin\tau \tag{34}$$

$$\frac{\partial\zeta}{\partial t} = u\sin\tau + \dot{z}\cos\tau - \dot{\theta}(a - s) \tag{35}$$

$$\dot{\tau} = \dot{\theta} \tag{36}$$

where τ is the equilibrium trim angle of the boat, and a is the value of s at the tranverse flow-plane through the boat center of gravity. From these equations and Equation (30) we have to the first order in the perturbations

[18] Pabst, W., "Landing Impact of Seaplanes," National Advisory Committee for Aeronautics TM 624 (1931).

$$\dot{\zeta} = U \sin \tau + u \sin \tau + \dot{z} \cos \tau - \dot{\theta} (a - s) \tag{37}$$

$$\ddot{\zeta} = 2 U \dot{\theta} \cos \tau + \dot{u} \sin \tau + \ddot{z} \cos \tau - \ddot{\theta} (a - s) \tag{38}$$

$$\frac{d\mu}{dt} = \dot{\zeta} \frac{\partial \mu}{\partial \zeta} = \dot{\zeta} \frac{\partial \mu}{\partial s} \cot \tau \tag{39}$$

On substituting these equations into Equation (32), dropping the second order perturbation terms, and integrating, we obtain

$$F_D = F_{DS} + \Delta F_D \tag{40}$$

where

$$F_{DS} = \varphi(\lambda) \mu_s U^2 \sin \tau \cos \tau \tag{41}$$

$$\Delta F_D = (2 F_{DS}/U)(u + \dot{z} \cot \tau + \dot{\theta} \ell_g / \sin \tau) + \varphi(\lambda) \left\{ (\dot{u} \sin \tau + \ddot{z} \cos \tau) \int_0^{\ell_k} \mu \, ds - \ddot{\theta} \int_0^{\ell_k} \mu (a - s) \, ds \right\} \tag{42}$$

The term μ_s is the value of the sectional added mass at the stern and $l_g = l_k - a$. The first term F_{DS} is the steady state hydrodynamic normal force, while the remaining terms ΔF_D are the linearized force contributions from surge, pitch, and heave perturbations in velocity and acceleration. The factor 2 multiplying the $\dot{z}$ and $\dot{\theta}$ terms in Equation (42) arises from the fact that the sectional added mass is not only a function of position on the hull but also of depth. This is represented by the contribution of $d\zeta/dt$ of Equation (35) to $d\mu/dt$ in Equation (39).

The hydrodynamic moment is obtained by integrating the product of the stripwise force in Equation (29) and the moment arm from the center of gravity a - s.

$$M_D = \varphi(\lambda) \int_0^{\ell_k} (a - s) \frac{d}{dt} (\mu \dot{\zeta}) \, ds \tag{43}$$

With the aid of Equations (31 through 39) we find from Equation (43), after dropping second order terms in the perturbations

$$M_D = M_{DS} + \Delta M_D \tag{44}$$

where

$$M_{DS} = \varphi(\lambda) U^2 \sin \tau \cos \tau \left[\int_0^{\ell_k} \mu \, ds - \ell_g \mu_s \right] \tag{45}$$

$$\Delta M_D = \frac{2 M_{DS}}{U} (u + \dot{z} \cot \tau)$$

$$- \varphi(\lambda) 2 U \cos \tau \left[\mu_s \ell_g^2 + \int_0^{\ell_k} \mu (a - s)\, ds \right] \ddot{\theta}$$

$$+ \varphi(\lambda) (\dot{u} \sin \tau + \ddot{z} \cos \tau) \int_0^{\ell_k} \mu (a - s)\, ds$$

$$- \varphi(\lambda) \ddot{\theta} \int_0^{\ell_k} \mu (a - s)^2\, ds \qquad (46)$$

The first term M_{DS} is the steady state hydrodynamic moment about the center of gravity of the boat. The remaining terms ΔM_D are the linearized contributions of the surge, pitch, and heave perturbations in velocity and acceleration.

VELOCITY AND ACCELERATION STABILITY DERIVATIVES

The vertical and horizontal components of the force stability derivatives with respect to the velocity and acceleration perturbations are the coefficients of the perturbation terms in the vertical and horizontal components of the perturbation force ΔF_D in Equation (42). We write these equations in nondimensional form* by dividing through by $1/2\, \rho U^2 b^2$. Thus the vertical component of the perturbation force equation becomes with Z positive down

$$\Delta Z_D = - 2 F_{DS}' \cos \tau \, (u' + \dot{z}' \cos \tau + \dot{\theta}' \lambda_g / \sin \tau)$$

$$- \varphi(\lambda) \left\{ (\dot{u}' \sin \tau \cos \tau + \ddot{z}' \cos^2 \tau) \int_0^{\lambda_k} \mu'\, ds' + \ddot{\theta}' \int_0^{\lambda_k} \mu' (a' - s')\, ds' \right\} \qquad (47)$$

where

$$F_{DS}' = \varphi(\lambda)\, \mu_s' \sin \tau \cos \tau$$

$$\lambda_k = \ell_k / b$$

$$\mu' = \mu / \tfrac{1}{2} \rho b^2$$

$$\dot{\theta}' = \dot{\theta}\, b/U \quad , \text{etc.} \qquad (48)$$

*Nondimensional quantities are represented by a prime symbol.

Likewise the horizontal component with X positive forward becomes

$$\Delta X_D' = \Delta Z_D' \tan \tau \tag{49}$$

The corresponding nondimensional stability derivatives for the moment equation are obtained in an analogous manner from the nondimensional form of Equation (46) as

$$\begin{aligned}\Delta M_D' &= 2 M_{DS}' (u' + \dot{z}' \cot \tau) \\ &\quad - \varphi(\lambda) 2 \cos \tau \left[\mu_s' \lambda_g^2 + \int_o^{\lambda_k} \mu' (a' - s') \, ds' \right] \dot{\theta}' \\ &\quad + \varphi(\lambda) (\dot{u}' \sin \tau + \ddot{z}' \cos \tau) \int_o^{\lambda_k} \mu' (a' - s') \, ds' \\ &\quad - \varphi(\lambda) \ddot{\theta}' \int_o^{\lambda_k} \mu' (a' - s')^2 \, ds'\end{aligned} \tag{50}$$

where

$$M_{DS}' = \varphi(\lambda) \int_o^{\lambda_k} \mu' (a' - s')^2 \, ds' \tag{51}$$

Typical notation for the nondimensional stability derivatives are shown as follows

$$Z_{\dot{\theta}}' = - 2 F_{DS} \lambda_g \cot \tau \qquad Z_{\ddot{z}}' = - \varphi(\lambda) \cos^2 \tau \int_o^{\lambda_k} \mu' \, ds'$$

$$X_u' = Z_u' \tan \tau \qquad X_{\dot{z}}' = Z_{\dot{z}}' \tan \tau$$

$$M_{\dot{\theta}}' = - \varphi(\lambda) \int_o^{\lambda_k} \mu' (a' - s')^2 \, ds' \qquad M_u' = 2 M_{DS}'$$

SECTIONAL ADDED MASS DISTRIBUTION

The next step is to find an expression for the distribution of the boat sectional added mass μ as a function of s. A general theoretical expression for this quantity is not available, even for prismatic hulls with constant deadrise. However, relatively simple approximate expressions for added mass have been used successfully in the past in the analysis of hydrodynamic impact of prismatic bodies.[16,17] For the sections of that portion of the body with the chines above the water surface, the sectional added mass was estimated by the following equation

$$\mu = \frac{\rho \pi \zeta^2}{2} f(\beta)^2 \tag{52}$$

where

$$f(\beta) = \frac{\pi}{2\beta} - 1 \tag{53}$$

β = deadrise angle in radians

This expression is based on the work of Wagner.[19] The quantity $\zeta f(\beta)$ is the radius of the semicircular cylinder representing the added mass of the section. For the sections of the hull with the chine submerged, the following expression was used.

$$\mu = \frac{\rho \pi b^2}{8} (f(\beta) \tan \beta)^2 + B \frac{\rho}{2} b(\zeta - \zeta_c) \tag{54}$$

where B is a function of the angle of deadrise, and b is the boat beam. The first term is the contribution of the V-shaped bottom alone at the instant of chine immersion. This is obtained from Equation (52) by putting $\zeta = \zeta_c = b/2 \tan \beta$. The second term is an estimate of the effect of chine depth as suggested by Schnitzer[17] and is based on the theory of Bobyleff[20] for infinite immersion. The Bobyleff function B is shown in Figure 22.

The expressions for μ given by Equations (52) and (54) will be used in Equations (40) and (44) to determine the normal force F_D and moment M_D. However, it is first necessary to define the range of keel length over which each contribution to μ is valid. It is clear that no single location, such as suggested by Equations (52) and (54), exists at which the effect of chine immersion starts, since the flow is much more complex than these equations suggest. This is especially true in the vicinity of chine immersion. However, a practical solution to this problem has been made possible by making the theory for the steady part of the normal force and moment consistent with the large amount of existing steady state data.

---

[19] Wagner, H., "The Phenomena of Impact and Planing on Water," National Advisory Committee for Aeronautics Translation 1366, ZAMM Bd 12, Heft 4, pp. 193 - 215 (Aug 1932).

[20] Lamb, H. "Hydrodynamics," Sixth Edition, Cambridge University Press, England (1932).

By assuming that the planing hull normal force at high speeds was made up of the sum of low-aspect-ratio wing lift and a cross flow drag term, Shuford[21] arrived at the basic form of an expression which he was able to fit very well to data obtained by many investigators.

These data cover a range of trim angles between 2 and 30 degrees, wetted lengths from one to seven beams, and deadrise angles between 0 and 50 degrees. His expression for the normal force is given by

$$F_{DS} = \frac{1}{2}\rho U^2 S\left[\frac{\pi A}{2(1+A)}\sin\tau\cos\tau\,(1-\sin\beta) + C_{D,c}\sin^2\tau\cos^2\tau\cos\beta\right] \tag{55}$$

where

$C_{D,c}$ = cross flow drag coefficient

S = planform area of the wetted portion of the hull or λb^2

A = aspect ratio of S, i.e.

$$A = b^2/S = 1/\lambda \tag{56}$$

The values of $C_{D,c}$ and the dependency on deadrise angle were obtained by a fit to the data. The cross flow drag coefficients were found to have the values shown in Table 2.[21]

TABLE 2 – CROSS FLOW DRAG COEFFICIENT[21]

Section shape	$C_{D,c}$
V-bottom, constant deadrise	1.33
V-bottom, horizontal chine flare	1.33 + 0.0147 β°
V-bottom, vertical chine strips	1.60 + 0.0147 β°

We will now define the various contributions μ_a to the sectional added mass along the hull by the following equations, which are somewhat less restrictive than Equations (52) and (54).

$$\mu_a = \begin{cases} \frac{\rho\pi}{2} f(\beta)^2 s^2 \tan^2\tau & o < s \leq s_{c1} \quad (57) \\ \frac{\rho\pi}{2} f(\beta)^2 s_{c1}^2 \tan^2\tau & s_{c1} < s \leq \ell_k \quad (58) \\ \frac{\rho}{2} B b \tan\tau\,(s - s_{c2}) & s_{c2} < s \leq \ell_k \quad (59) \end{cases}$$

[21] Shuford, C.L., Jr., "A Theoretical and Experimental Study of Planing Surfaces Including Effects of Cross Section and Plan Form," National Advisory Committee for Aeronautics Report 1355, (1957).

where we have made the substitution

$$\zeta = s \tan \tau \tag{60}$$

The sectional added mass μ at any section is simply the sum of the contributions at that section. The principle difference from Equations (52) and (54) is that s_{c1} and s_{c2} have not been assumed to be known in advance. Equations (57) and (58) are the contributions from the bottom of the hull to the chine. The quantity s_{c1} is the value of s at the point where the chine is effectively immersed. Equation (59) is the contribution corresponding to the second term in Equation (54), and s_{c2} is the value of s at which this begins to grow.

From Equations (57 through 59) we readily find that

$$\mu_s = \frac{\rho\pi}{2} (f(\beta)\, s_{c1} \tan \tau)^2 + \frac{\rho}{2} B\, b \tan \tau\, (\ell_k - s_{c2}) \tag{61}$$

$$\int_0^{\ell_k} \mu\, ds = \frac{\rho\pi}{2} (f(\beta)\, s_{c1} \tan \tau)^2 \left(\ell_k - \frac{2}{3} s_{c1}\right) + \frac{\rho}{2} B\, b \tan \tau \frac{(\ell_k - s_{c2})^2}{2} \tag{62}$$

Substituting Equation (61) into Equation (41) gives

$$F_{DS} = \frac{\rho U^2}{2} [\varphi(\beta)\pi (f(\beta)\, s_{c1} \tan \tau)^2 \sin \tau \cos \tau$$

$$+ \varphi(\lambda)\, B\, b \sin^2 \tau\, (\ell_k - s_{c2})] \tag{63}$$

This equation becomes identical with the formulation of Shuford in Equation (55) provided

$$\phi(\lambda) = \frac{\lambda}{1 + \lambda} = \frac{1}{1 + A} \tag{64}$$

$$\frac{\rho\pi}{2} (f(\beta)\, s_{c1} \tan \tau)^2 = \frac{\rho\pi b^2}{4} (1 - \sin \beta) \tag{65}$$

$$\varphi(\lambda)\, B = C_{D,c} \cos^2 \tau \cos \beta \tag{66}$$

$$\ell_k - s_{c2} = \lambda\, b \tag{67}$$

The three-dimensional correction factor of Equation (64) has a trend similar to the result obtained by Pabst as shown by Figure 21. Also the variation of B with deadrise angle is seen to be proportional to cos β in Figure 22.

If we substitute Equations (64) through (67) into Equation (63) and nondimensionalize, we obtain

$$F_{DS}' = \frac{\lambda}{1 + \lambda} \frac{\pi}{2} \sin \tau \cos \tau\, (1 - \sin \beta)$$

$$+ C_{D,c}\, \lambda \sin^2 \tau \cos^2 \tau \cos \beta \tag{68}$$

Likewise if we substitute Equations (61) through (67) into Equation (45) and divide by $1/2\ \rho\ U^2\ b^3$ we obtain the nondimensional dynamic moment about the center of gravity

$$M_{DS}' = \frac{\lambda}{1+\lambda}\ \frac{\pi}{2} \sin\tau \cos\tau\ (1 - \sin\beta)\left(\lambda_k - \frac{2}{3}\lambda_{c1} - \lambda_g\right)$$

$$+ C_{D,c} \sin^2\tau \cos^2\tau \cos\beta\left(\frac{\lambda}{2} - \lambda_g\right)\lambda \qquad (69)$$

where $\lambda_{c1} = s_{c1}/b$

$\lambda_{c2} = s_{c2}/b$

$\lambda_g = \ell_g/b$

$\lambda_k = \ell_k/b$

DETERMINATION OF λ_{c1}, λ_{c2}, λ_k

Because of wave rise on impact, the effective depth of the V-bottom is greater than the depth relative to the calm water free surface. Wagner[19] found that before chine immersion, the effective depth was greater by a factor of $\pi/2$. Therefore the effective radius c of the semicircular cylinder of water representing $\mu(s)$ is taken as

$$c = \frac{\pi}{2}\, s\, \frac{\tan\tau}{\tan\beta} \qquad (70)$$

Combining with Equation (57) gives

$$\mu(s) = \rho\,\frac{\pi}{2}\,c^2\left[\left(1 - \frac{2\beta}{\pi}\right)^2 \frac{\tan^2\beta}{\beta^2}\right] \qquad \text{for } s \leq s_{c1} \qquad (71)$$

The factor in brackets represents the effect of deadrise angle on the sectional added mass. Shuford found that this did not correlate well with data for angles of deadrise greater than 25 degrees. He therefore substituted the function $(1 - \sin\beta)$ which correlated well with data to $\beta = 50$ degrees. Making this substitution in Equation (71) and substituting into Equation (65) we find the following expression for c

$$c = \sqrt{2}\left(\frac{b}{2}\right) \qquad \text{for } s = s_{c1} \qquad (72)$$

This equation is seen to be independent of deadrise angle. On substituting into Equation (70), we obtain

$$s_{c1} = \frac{\sqrt{2}}{\pi}\,\frac{\tan\beta}{\tan\tau}\,b = \lambda_{c1}\,b \qquad (73)$$

An expression for the mean wetted length-to-beam ratio λ has been obtained by Brown[10] from extensive photographic observations as

$$\lambda = 0.5\,(\lambda_k + \lambda_c) + 0.03 \tag{74}$$

where λ_c, the ratio of the wetted length of chine to beam, is

$$\lambda_c = \lambda_k - (0.57 + 0.001\,\beta)(\tan\beta/(2\tan\tau) - 0.006\,\beta) \tag{75}$$

provided $\lambda_c \geq 1$. The last term in Equation (74) is an allowance for stagnation line curvature. We then find from the previous equations that

$$\lambda_{c2} = 0.5\,(0.57 + 0.001\,\beta)(\tan\beta/(2\tan\tau) - 0.006\,\beta) - 0.03 \tag{76}$$

since according to Equation (67)

$$\lambda_k = \lambda + \lambda_{c2} \tag{77}$$

Equations (73), (76), and (77) completely define the ranges of the sectional added mass distributions in terms of β, λ, and τ. Both λ and τ are obtained from the steady state equilibrium conditions to be discussed in a later section.

It is noted that the value of λ_{c2} as defined by Equations (59) and (76) is smaller than $\lambda_k - \lambda_c$ which corresponds to the lower limit of integration at which $\zeta = \zeta_c$ in the representation of the second term of the added mass in Equation (54). Although it appears more reasonable to use $\lambda_k - \lambda_c$ for the lower limit of integration, the best fit to the data[10] requires that we use the λ_{c2} of Equation (76). In the numerical analysis, the effect of using $\lambda_k - \lambda_c$ in place of λ_{c2} was found to be insignificant except for the 20-degree-deadrise case. Calculations of τ_c using $\lambda_k - \lambda_c$ are shown by the broken curves in Figure 6 where it is seen to produce a small improvement in the fit to the data.

ADDED MASS FUNCTIONS

The added mass functions used in evaluating the stability derivatives may now be expressed in terms of the hull geometry and the integration limits λ_{c1}, λ_{c2}, and λ_k.

The nondimensional sectional added mass at the stern, including the three-dimensional effects is readily obtained from Equations (61) and (64) through (67) as

$$\varphi(\lambda)\,\mu_s' = 2(P + Q) \tag{78}$$

where

$$P = \frac{\pi}{4}\,\frac{\lambda}{1+\lambda}\,(1 - \sin\beta)$$

$$Q = \frac{C_{D,c}}{2} \lambda \sin \tau \cos \tau \cos \beta$$

The nondimensional added mass in heave is, from Equation (62)

$$\varphi(\lambda) \int_0^{\lambda_k} \mu' \, ds' = 2P\chi_4 + Q\lambda \tag{79}$$

where

$$\chi_4 = \lambda_k - \frac{2}{3}\lambda_{c1}$$

The nondimensional first moment of the added mass with respect to the point s = 0 is readily obtained with the aid of Equations (57) through (59) as

$$\varphi(\lambda) \int_0^{\lambda_k} \mu' \, s' \, ds' = 2\left(P\chi_2 + \frac{Q}{\lambda}\chi_3\right) \tag{80}$$

where

$$\chi_2 = \frac{\lambda_k^2}{2} - \frac{\lambda_{c1}^2}{4}$$

$$\chi_3 = \frac{\lambda_k^3 - \lambda_{c2}^3}{3} - \left(\frac{\lambda_k^2 - \lambda_{c2}^2}{2}\right)\lambda_{c2}$$

The nondimensional second moment of the added mass with respect to the point s = 0 is

$$\varphi(\lambda) \int_0^{\lambda_k} \mu' \, s'^2 \, ds' = 2\left(P\chi_5 + \frac{Q}{\lambda}\chi_6\right) \tag{81}$$

where

$$\chi_5 = \frac{\lambda_{c1}^3}{5} + \frac{\lambda_k^3 - \lambda_{c1}^3}{3}$$

$$\chi_6 = \frac{\lambda_k^4 - \lambda_{c2}^4}{4} - \left(\frac{\lambda_k^3 - \lambda_{c2}^3}{3}\right)\lambda_{c2}$$

REMAINING FORCE AND MOMENT CONTRIBUTIONS

To completely specify the forces and moments on a planing craft, it is necessary to add to Equations (40) and (44) the contributions due to perturbations in pitch and heave displacement, buoyancy, skin friction, thrusters, aerodynamic factors, and towing forces and moments. Although the thrusters may have a significant effect on the equilibrium trim and wetted length, their effect on the stability derivatives is probably not very large. In any event these effects

may be estimated by means of existing techniques,[22,23] and will not be considered further here. However, the effect of a towing force and moment will be included in order to facilitate comparison with towed model data.

The contributions due to perturbations in pitch and heave displacement may readily be obtained from the complete expressions for the steady state force and moment. The additional terms required to complete these expressions are described as follows.

BUOYANCY FORCE AND MOMENT

We will consider only the cases for speed coefficient C_V greater than 0.5, where the water breaks clear of the transom, thus fully ventilating the backside of the boat to the atmosphere. For this case the hydrostatic force may be assumed to act normal to the keel. The following expression was found to fit the data reasonably well.[10,24]

$$F_{BS}' = \kappa \lambda^2 \sin \tau / C_V^2 \tag{82}$$

where κ is an empirical correction factor which accounts for ventilation effects on the static pressure. On the basis of preliminary analysis of planing boat test data, a value of κ of 0.7 was tentatively suggested by Hsu.[24] However, from recent extensive experiments with a 10-degree deadrise prismatic planing hull, Brown[10] obtained the best agreement with the data by putting

$$\kappa = 0.624 \tag{83}$$

and assuming that it acts at one third of the mean wetted length from the stern. Since the present analysis deals with prismatic hulls Equation (83) will be used in the following. The moment about the center of gravity is clearly

$$M_{BS}' = F_{BS}' \left(\frac{\lambda}{3} - \lambda_g \right) \tag{84}$$

SKIN FRICTION

The contribution due to skin friction is assumed to act tangential to the bottom and mid-way between the keel and chine lines. It is given in terms of the mean wetted area by Savitsky[5]

---

[22] Hadler, J.B., "The Prediction of Power Performance on Planing Craft," Transactions Society of Naval Architects and Marine Engineers, Vol. 74, pp. 563 - 610 (1966).

[23] Ribner, H.S., "Propellers in Yaw," National Advisory Committee for Aeronautics Report 820 (1949).

[24] Hsu, C.C., "On the Motions of High Speed Planing Craft," Hydronautics Report 603-1 (May 1967).

$$F_{FS}' = \lambda C_f/\cos\beta \tag{85}$$

where the friction coefficient C_f is given by

$$\frac{0.242}{\sqrt{C_f}} = \log_{10}\left[C_f\left(\frac{U\lambda b}{\nu}\right)\right]$$

as a function of Reynolds number. The moment about the center of gravity is clearly

$$M_{FS}' = - F_{FS}'\left(\lambda_v - \frac{\tan\beta}{4}\right) \tag{86}$$

TOWING AND AERODYNAMIC FORCES

Terms similar to the above Equation (86) may be written for the towing and aerodynamic force and moment contributions. These are assumed here to act in a line parallel to the steady part of the straight line motion.* The moments about the center of gravity, due to the tow force T_S' and wind force F_{WS}', respectively, are

$$M_{TS}' = - T_S' f(k_1, e_1) \tag{87}$$

$$M_{WS}' = F_{WS}' f(k_2, e_2) \tag{88}$$

where

$f(k_n, e_n) = (\lambda_{kn} - \lambda_v)\cos\tau + (\lambda_{en} - \lambda_g)\sin\tau$

$\lambda_{k1}, \lambda_{e1}$ = nondimensional coordinates of the towpoint with respect to keel at the stern; see Figure 23

$\lambda_{k2}, \lambda_{e2}$ = coordinates of the resultant windforce

λ_v = perpendicular distance from the keel to the center of gravity

STEADY STATE EQUILIBRIUM

The steady state trim angle τ and mean wetted length λb are readily determined from the steady state force and moment equations. The force equation is resolved into a vertical (lift) component and a horizontal (drag) component. The lift equation is readily obtained by setting the boat weight W equal to the sum of the vertical component of the various force contributions defined earlier. Thus in nondimensional form we have

$$W' = - Z_S' = (F_{DS}' + F_{BS}')\cos\tau - F_{FS}'\sin\tau \tag{89}$$

*This is a good assumption for the model experiments discussed later.

where Z_S' is the nondimensional hydrodynamic lift, positive down. Similarly the nondimensional tow force F_{TS}' is set equal to the drag or horizontal component of the force contributions.

$$T_S' = - X_S' = (F_{DS}' + F_{BS}') \sin \tau + F_{FS}' \cos \tau + F_{WS}'$$

$$= - Z_S' \tan \tau + F_{FS}'/\cos \tau + F_{WS}' = D_S' \tag{90}$$

where D_S' is the nondimensional drag of the boat. The moment equation is obtained by summing the components

$$M_S' = M_{DS}' + M_{BS}' + M_{FS}' + M_{TS}' + M_{WS}' = 0 \tag{91}$$

where the component moments are given with respect to the center of gravity.

If we substitute Equations (68), (82), and (85) into Equation (89) we obtain finally for the steady state lift equation

$$W' = - Z_S' = \frac{\lambda}{1 + \lambda} \frac{\pi}{2} \sin \tau \cos^2 \tau (1 - \sin \beta) + C_{D,c} \lambda \sin^2 \tau \cos^3 \tau \cos \beta$$

$$+ \frac{0.624}{C_V^2} \lambda^2 \sin \tau \cos \tau - \lambda C_f \sin \tau/\cos \beta \tag{92}$$

If we multiply this equation by $1 + \lambda$ we obtain the following form of Equation (92) as a cubic equation in λ.

$$D\lambda^3 + (C + D + E) \lambda^2 + (B + C - E - W') \lambda - W' = 0 \tag{93}$$

where

$$B = \frac{\pi}{2} \sin \tau \cos^2 \tau (1 - \sin \beta)$$

$$C = C_{D,c} \sin^2 \tau \cos^3 \tau \cos \beta$$

$$D = 0.624 \sin \tau \cos \tau/C_V^2$$

$$E = - C_f \sin \tau/\cos \beta \tag{94}$$

Substituting Equations (69), (77), (84), (86), (87), (88), and (90) into Equation (91) yields

$$M_S' = \frac{\pi}{4} \frac{\sin 2\tau (1 - \sin \beta) \lambda}{1 + \lambda} (\lambda + h(\tau) - \lambda_g) + C_{D,c} (\sin 2\tau)^2 \cos \beta \left(\frac{\lambda}{2} - \lambda_g\right) \frac{\lambda}{4}$$

$$+ \frac{0.624 \sin \tau}{C_V^2} \lambda^2 \left(\frac{\lambda}{3} - \lambda_g\right) - \frac{C_f}{\cos \beta} \lambda \left(\lambda_v - \frac{\tan \beta}{4}\right)$$

$$+ \left(Z_S' \tan \tau - \frac{- \lambda C_f}{\cos \tau \cos \beta} - F_{WS}'\right) f(k_1, e_1) + F_{WS}' f(k_2, e_2) = 0 \tag{95}$$

where

$$h(\tau) = \lambda_{c2} - \frac{2}{3}\lambda_{c1} \tag{96}$$

Equations (93) and (95) must be solved for λ and τ by an iterative procedure in which successive values of τ are assumed. Equation (93) is solved for λ for each assumed value of τ. Successive pairs of λ and τ thus determined are substituted into Equation (95) until its magnitude becomes equal to zero within some prespecified amount. In the present analysis this was taken as $0.002/C_V^2$.

STATIC STABILITY DERIVATIVES

As noted earlier the force and moment stability derivatives with respect to the heave and pitch velocity and acceleration perturbations are readily obtained from Equations (47) and (50). There only remains the task of obtaining the derivatives with respect to the heave and pitch angle displacement perturbations. These are readily obtained with the aid of the expressions for Z_S' and M_S' in Equations (92) and (95). Since, for a given deadrise and speed, they are functions only of $\lambda(z', \tau)$ and τ we have for the derivatives with respect to the heave and pitch perturbations

$$\frac{\partial Z'}{\partial z'} = \frac{\partial Z_S'}{\partial \lambda}\frac{\partial \lambda}{\partial z'} \tag{97}$$

$$\frac{\partial X'}{\partial z'} = \frac{\partial X_S'}{\partial \lambda}\frac{\partial \lambda}{\partial z'} \tag{98}$$

$$\frac{\partial M'}{\partial z'} = \frac{\partial M_S'}{\partial \lambda}\frac{\partial \lambda}{\partial z'} \tag{99}$$

$$\frac{\partial Z'}{\partial \theta} = \frac{\partial Z_S'}{\partial \tau} + \frac{\partial Z_S'}{\partial \lambda}\frac{\partial \lambda}{\partial \tau} \tag{100}$$

$$\frac{\partial X'}{\partial \theta} = \frac{\partial X_S'}{\partial \tau} + \frac{\partial X_S'}{\partial \lambda}\frac{\partial \lambda}{\partial \tau} \tag{101}$$

$$\frac{\partial M'}{\partial \theta} = \frac{\partial M_S'}{\partial \tau} + \frac{\partial M_S'}{\partial \lambda}\frac{\partial \lambda}{\partial \tau} \tag{102}$$

where all rotations are with respect to the center of gravity; $z' = z/b$ and z equals perturbation in heave displacement, positive down. From Equations (90), (92), and (95) we readily find

$$\frac{\partial Z_S'}{\partial \lambda} = - G \sin \tau \left(\frac{\cos \tau}{1 + \lambda}\right)^2 - H \sin^2 \tau \cos^3 \tau$$

$$- 2 J \sin \tau \cos \tau \lambda + C_f \sin \tau / \cos \beta \qquad (103)$$

$$\frac{\partial Z_S'}{\partial \tau} = - G \frac{\lambda}{1 + \lambda} (\cos^3 \tau - 2 \sin^2 \tau \cos \tau)$$

$$- H\lambda (2 \sin \tau \cos^4 \tau - 3 \cos^2 \tau \sin^3 \tau)$$

$$- J\lambda^2 \cos 2\tau + C_f \lambda \cos \tau / \cos \beta \qquad (104)$$

$$\frac{\partial X_S'}{\partial \lambda} = \frac{\partial Z_S'}{\partial \lambda} \tan \tau + \frac{\partial F_{FS}'}{\partial \lambda} \frac{1}{\cos \tau} \approx \frac{\partial Z_S'}{\partial \lambda} \tan \tau \qquad (105)$$

$$\frac{\partial X_S'}{\partial \tau} = \frac{\partial Z_S'}{\partial \tau} \tan \tau + \frac{Z_S'}{\cos^2 \tau} + \frac{F_{FS}' \tan \tau}{\cos \tau} \approx \frac{\partial Z_S'}{\partial \tau} \tan \tau + \frac{Z_S'}{\cos^2 \tau} \qquad (106)$$

$$\frac{\partial M_S'}{\partial \lambda} = G \sin \tau \cos \tau \left[\left(\frac{1}{1 + \lambda}\right)^2 (\lambda + h(\tau) - \lambda_g) + \frac{\lambda}{1 + \lambda}\right]$$

$$+ H \sin^2 \tau \cos^2 \tau (\lambda - \lambda_g) + J \sin \tau \lambda (\lambda - 2\lambda_g)$$

$$+ \frac{C_f}{\cos \beta} \left(\frac{\tan \beta}{4} - \lambda_v\right) + \left(\frac{\partial Z_S'}{\partial \lambda} \tan \tau - \frac{C_f}{\cos \beta \cos \tau}\right) f(k_1, e_1) \qquad (107)$$

$$\frac{\partial M_S'}{\partial \tau} = G \frac{\lambda}{1 + \lambda} \left[\cos 2\tau (\lambda + h(\tau) - \lambda_g) + (0.157 - 0.00025 \beta) \frac{\tan \beta}{\tan \tau}\right]$$

$$+ H\lambda \left(\frac{\lambda}{2} - \lambda_g\right) \sin 2\tau \cos 2\tau + J\lambda^2 \left(\frac{\lambda}{3} - \lambda_g\right) \cos \tau$$

$$+ \left(\frac{\partial Z_S'}{\partial \tau} \tan \tau + \frac{Z_S'}{\cos^2 \tau} - \frac{C_f \lambda \tan \tau}{\cos \beta \cos \tau}\right) f(k_1, e_1)$$

$$- \left(Z_S' \tan \tau - \frac{C_f \lambda}{\cos \beta \cos \tau} - F_{WS}'\right) g(k_1, e_1) - F_{WS}' g(k_2, e_2) \qquad (108)$$

where

$$g(k_n, e_n) = (\lambda_{kn} - \lambda_v) \sin \tau - (\lambda_{en} - \lambda_g) \cos \tau$$

$$G = \pi (1 - \sin \beta)/2$$

$$H = C_{D,c} \cos \beta$$

$$J = 0.624/C_V^2 \qquad (109)$$

Also with the aid of Equations (76) and (77) and Figure 20 it is easy to show that

$$\frac{\partial \lambda}{\partial z'} = \frac{1}{\sin \tau} \tag{110}$$

$$\frac{\partial \lambda}{\partial \tau} = -\left(\frac{\lambda_k - \lambda_g}{\tan \tau} + \lambda_v\right) + (0.57 + 0.001\,\beta)\frac{\tan \beta}{4 \sin^2 \tau} \tag{111}$$

STABILITY EQUATIONS

The total nondimensional force and moment equations may now be written as

$$m' \dot{u}' = T_S' + X_S' + \Delta X_D' + \frac{\partial X'}{\partial z'} + \frac{\partial X'}{\partial \theta} + \Delta T_S' \tag{112}$$

$$m' \ddot{z}' = W' + Z_S' + \Delta Z_D' + \frac{\partial Z'}{\partial z'} + \frac{\partial Z'}{\partial \theta} \tag{113}$$

$$I_y' \ddot{\theta}' = M_S' + \Delta M_D' + \frac{\partial M'}{\partial z'} + \frac{\partial M'}{\partial \theta} \tag{114}$$

where

$$m' = \frac{m}{\frac{1}{2}\rho b^3} = \text{nondimensional mass of the boat}$$

$$I' = \frac{I_y}{\frac{1}{2}\rho b^5} = \text{nondimensional pitch moment of inertia about the center of gravity}$$

$$\Delta T_S' = \frac{\Delta T_S}{\frac{1}{2}\rho U^2 b^2} = \text{perturbation in tow force}$$

From the static equilibrium Equations (89) through (91) we require that

$$\begin{aligned} T_S' + X_S' &= 0 \\ W' + Z_S' &= 0 \\ M_S' &= 0 \end{aligned} \tag{115}$$

If the body is free to surge then $\Delta T_S'$ is zero. If the body is restrained in surge u' and $\dot{u}'$ are zero, and the pitch and heave motions are uncoupled from surge.

Assuming that the body is free to surge, the stability equations at the equilibrium flying conditions are obtained by putting $\Delta T_S'$ equal to zero and substituting Equations (47), (49), (50), and (115) into Equations (112) through (114). This leads to the following equations

where the primes have been omitted for convenience.

$$(X_{\dot{u}} - m)\dot{u} + X_u u + X_{\ddot{z}}\ddot{z} + X_{\dot{z}}\dot{z} + X_z z + X_{\ddot{\theta}}\ddot{\theta} + X_{\dot{\theta}}\dot{\theta} + X_\theta \theta = 0 \tag{116}$$

$$Z_{\dot{u}}\dot{u} + Z_u u + (Z_{\ddot{z}} - m)\ddot{z} + Z_{\dot{z}}\dot{z} + Z_z z + Z_{\ddot{\theta}}\ddot{\theta} + Z_{\dot{\theta}}\dot{\theta} + Z_\theta \theta = 0 \tag{117}$$

$$M_{\dot{u}}\dot{u} + M_u u + M_{\ddot{z}}\ddot{z} + M_{\dot{z}}\dot{z} + M_z z + (M_{\ddot{\theta}} - I_y)\ddot{\theta} + M_{\dot{\theta}}\dot{\theta} + M_\theta \theta = 0 \tag{118}$$

where the force derivatives are

$$Z_{\dot{u}} = -\varphi(\lambda)\sin\tau\cos\tau\int \mu'\,ds' \qquad X_{\dot{u}} = Z_{\dot{u}}\tan\tau$$

$$Z_u = -2\varphi(\lambda)\mu_s'\sin\tau\cos^2\tau \qquad X_u = Z_u\tan\tau$$

$$Z_{\ddot{z}} = -\varphi(\lambda)\cos^2\tau\int \mu'\,ds' \qquad X_{\ddot{z}} = Z_{\ddot{z}}\tan\tau$$

$$Z_{\dot{z}} = -2\varphi(\lambda)\mu_s'\cos^3\tau \qquad X_{\dot{z}} = Z_{\dot{z}}\tan\tau$$

$$Z_z = \frac{\partial Z_S'}{\partial\lambda}\frac{\partial\lambda}{\partial z'} \qquad X_z = Z_z\tan\tau$$

$$Z_{\ddot{\theta}} = -\varphi(\lambda)\int \mu'(a' - s')\,ds' \qquad X_{\ddot{\theta}} = Z_{\ddot{\theta}}\tan\tau$$

$$Z_{\dot{\theta}} = -2\varphi(\lambda)\mu_s'\lambda_g\cos^2\tau \qquad X_{\dot{\theta}} = Z_{\dot{\theta}}\tan\tau$$

$$Z_\theta = \frac{\partial Z_S'}{\partial\tau} + \frac{\partial Z_S'}{\partial\lambda}\frac{\partial\lambda}{\partial\tau} \qquad X_\theta = Z_\theta\tan\tau + \frac{Z_S'}{\cos^2\tau} \tag{119}$$

and the moment derivatives are

$$M_{\dot{u}} = \varphi(\lambda)\sin\tau\int \mu'(a' - s')\,ds'$$

$$M_u = 2\varphi(\lambda)\sin\tau\cos\tau\left(\int \mu'\,ds' - \lambda_g\mu_s'\right)$$

$$M_{\ddot{z}} = \varphi(\lambda)\cos\tau\int \mu'(a' - s')\,ds'$$

$$M_{\dot{z}} = 2\varphi(\lambda)\cos^2\tau\left(\int \mu'\,ds' - \lambda_g\mu_s'\right)$$

$$M_z = \frac{\partial M_S'}{\partial\lambda}\frac{\partial\lambda}{\partial z'}$$

$$M_{\ddot{\theta}} = -\varphi(\lambda)\int \mu'(a' - s')^2\,ds'$$

$$M_{\dot{\theta}} = -2\varphi(\lambda)\cos\tau\left(\mu_s'\lambda_g^2 + \int \mu'(a' - s')\,ds'\right)$$

$$M_\theta = \frac{\partial M_S'}{\partial\tau} + \frac{\partial M_S'}{\partial\lambda}\frac{\partial\lambda}{\partial\tau} \tag{120}$$

The integrations are from 0 to λ_k. The evaluation of the added mass terms are readily obtained with the aid of Equations (78) through (81). The static derivatives are given by Equations (97) through (108). The expressions for F_{DS}' and M_{DS}' are given by Equations (68) and (69).

It is seen from Equation (119) that for small trim angles the derivatives of the X-equation are considerably smaller than those of the Z-equation. Under these conditions it is reasonable to expect that the influence of the surge degree of freedom on the porpoising stability would be small enough so that the X-equation could be omitted. In any case, if the boat is being towed at constant speed, then, as previously noted, values of u and $\dot{u}$ in Equations (117) and (118) are zero. This effectively uncouples the surge degree of freedom, and the stability may be determined from the pitch and heave equations alone. In the present investigation, all of the data available for checking the theory were obtained by using planing boat models towed at constant speed. For these reasons numerical calculations have been made using only the pitch and heave stability equations.

APPENDIX B

ESTIMATES OF EFFECT OF WINDAGE AND CHINE RADIUS ON STABILITY DERIVATIVES

A high metal framework was attached to the models of Day and Haag.[4] Its purpose was to support a scribe for recording the motion after the boat started to porpoise. This introduced a small aerodynamic drag and moment on the model. The following estimated values for this drag were used in the computations

$$F_{WS}' = 0.0032$$

$$\lambda_{e2} = 1.3$$

$$\lambda_{k2} = 2.6$$

Shuford[21] found that a small radius on the chine will account for a reduction in lift of 5 to 10 percent - corresponding to a 1/64- and 1/16-inch radius, respectively, on a 4-inch-beam, flat-bottom, planing surface. On the basis of chine radius measurements obtained from a typical wood model, it was estimated that the models used by Day and Haag had about a 5 percent loss in dynamic lift. The theoretical calculations were therefore modified to take this into account. This amounted to reducing the magnitude of P and Q in Equations (78) through (81) and G and H in Equations (103) through (108) by 5 percent.

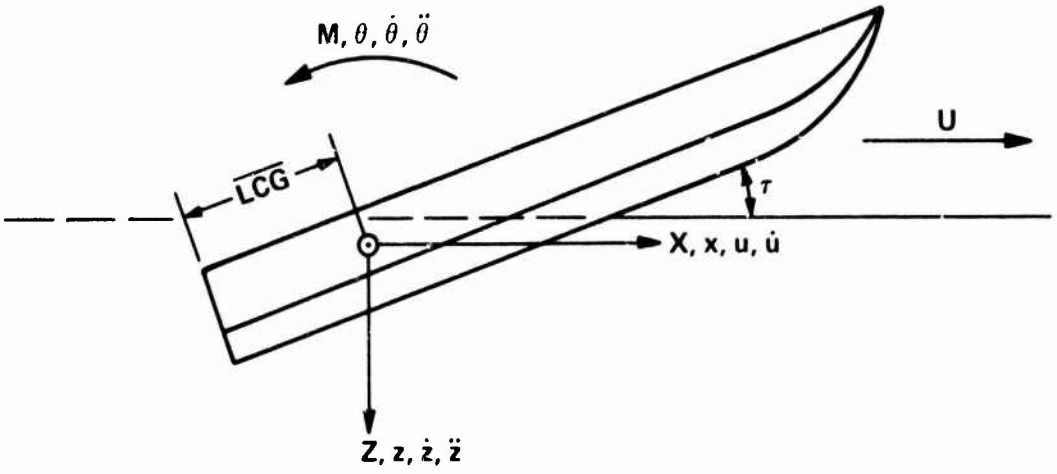

Figure 1 – Coordinate System

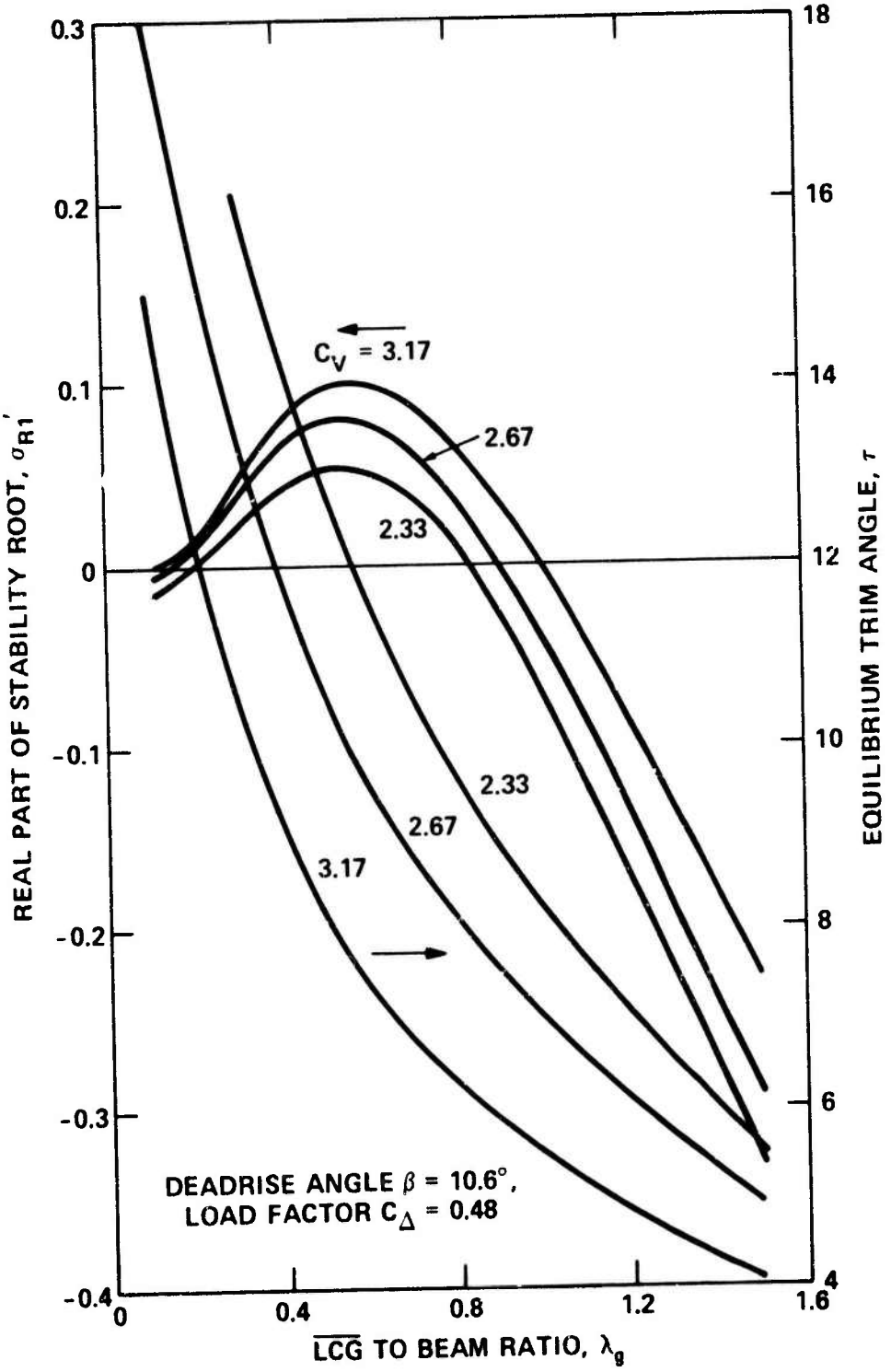

Figure 2 – Variation of Least Stable Real Root and Trim Angle with Position of Center of Gravity

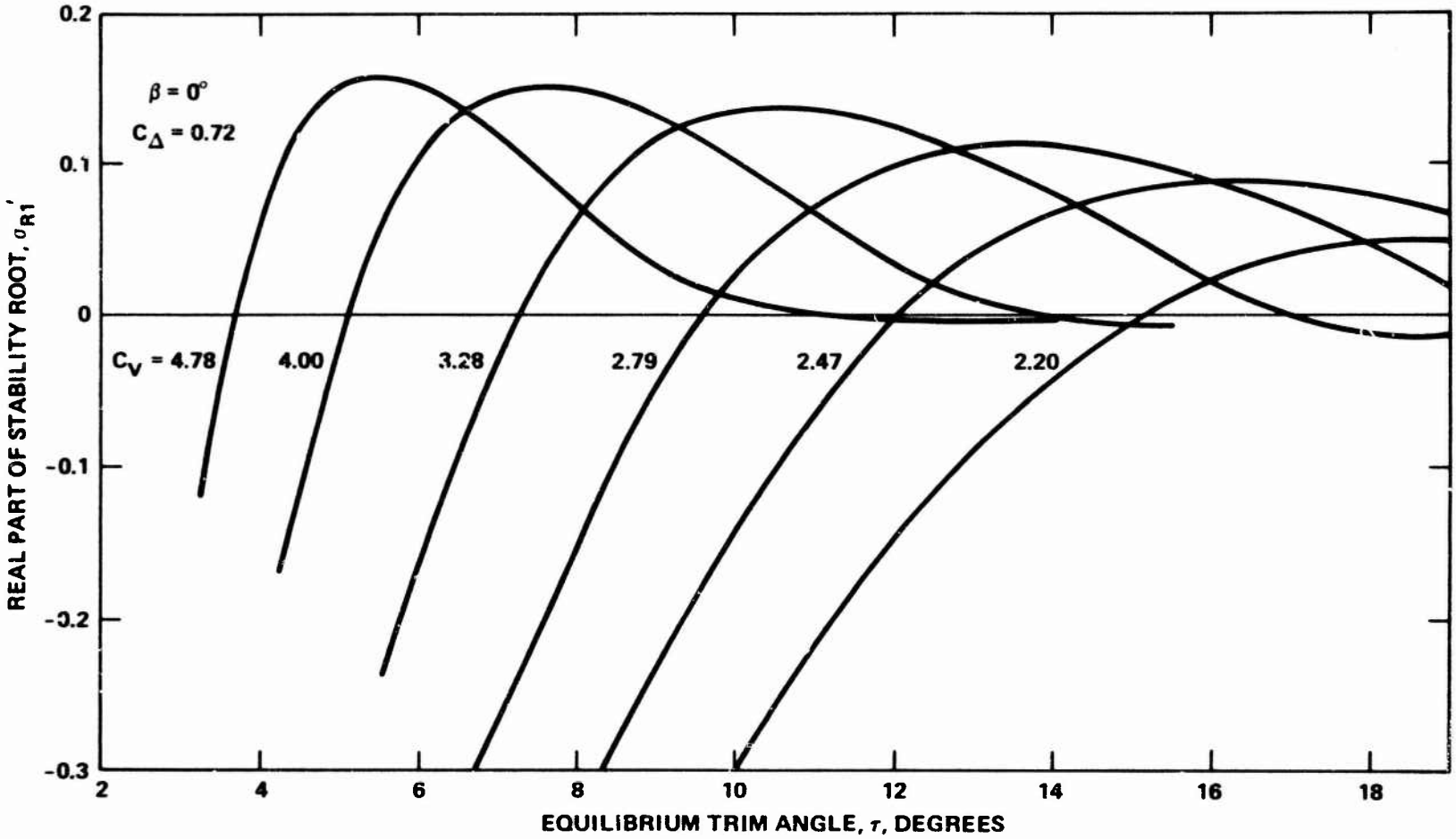

Figure 3 – Variation of Stability Root with Trim Angle for Various Values of Speed Coefficient, Deadrise Angle of 0 Degree, Load Coefficient of 0.72

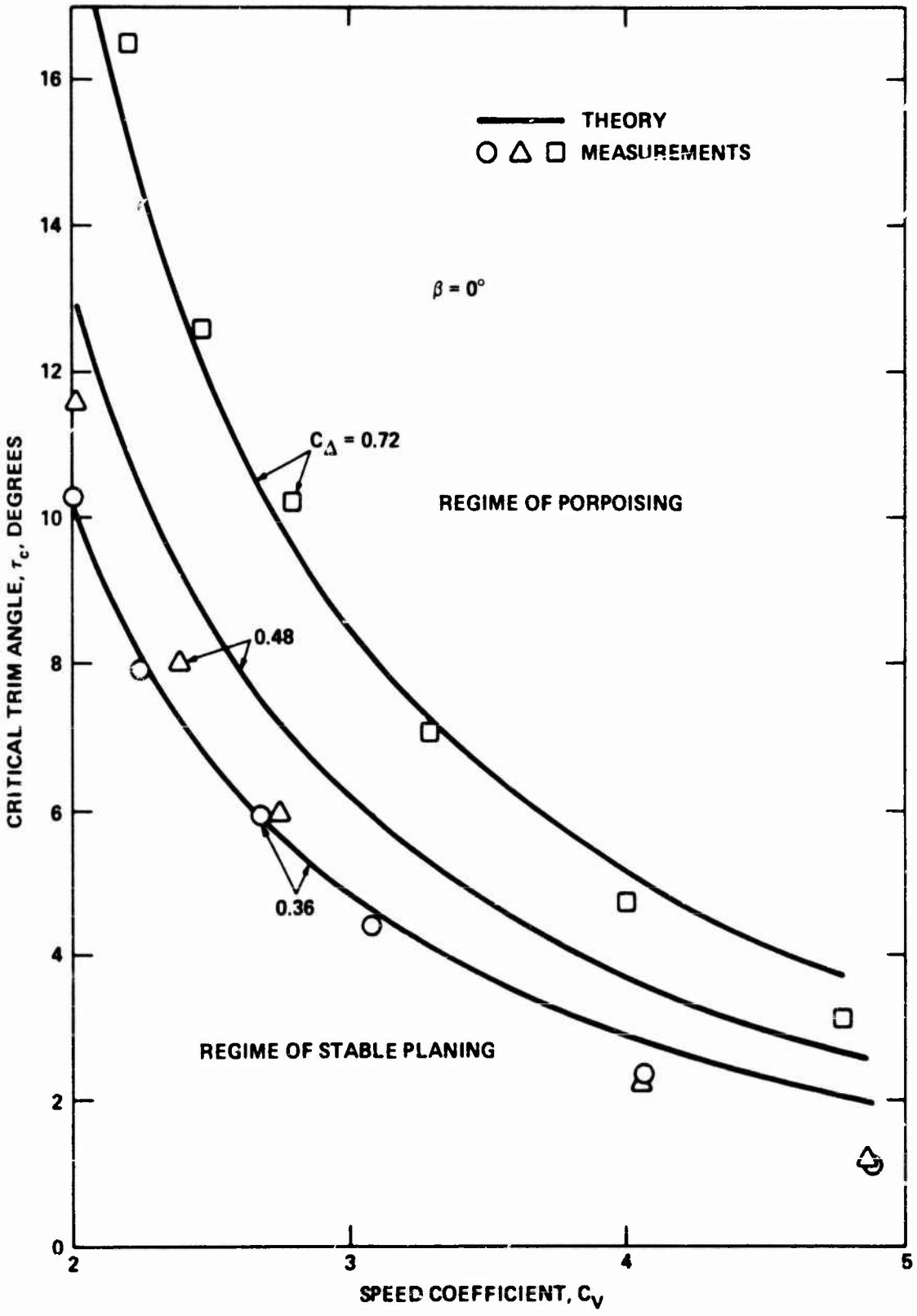

Figure 4 – Comparison of Theoretical and Measured Porpoising Boundaries for Deadrise of 0 Degree

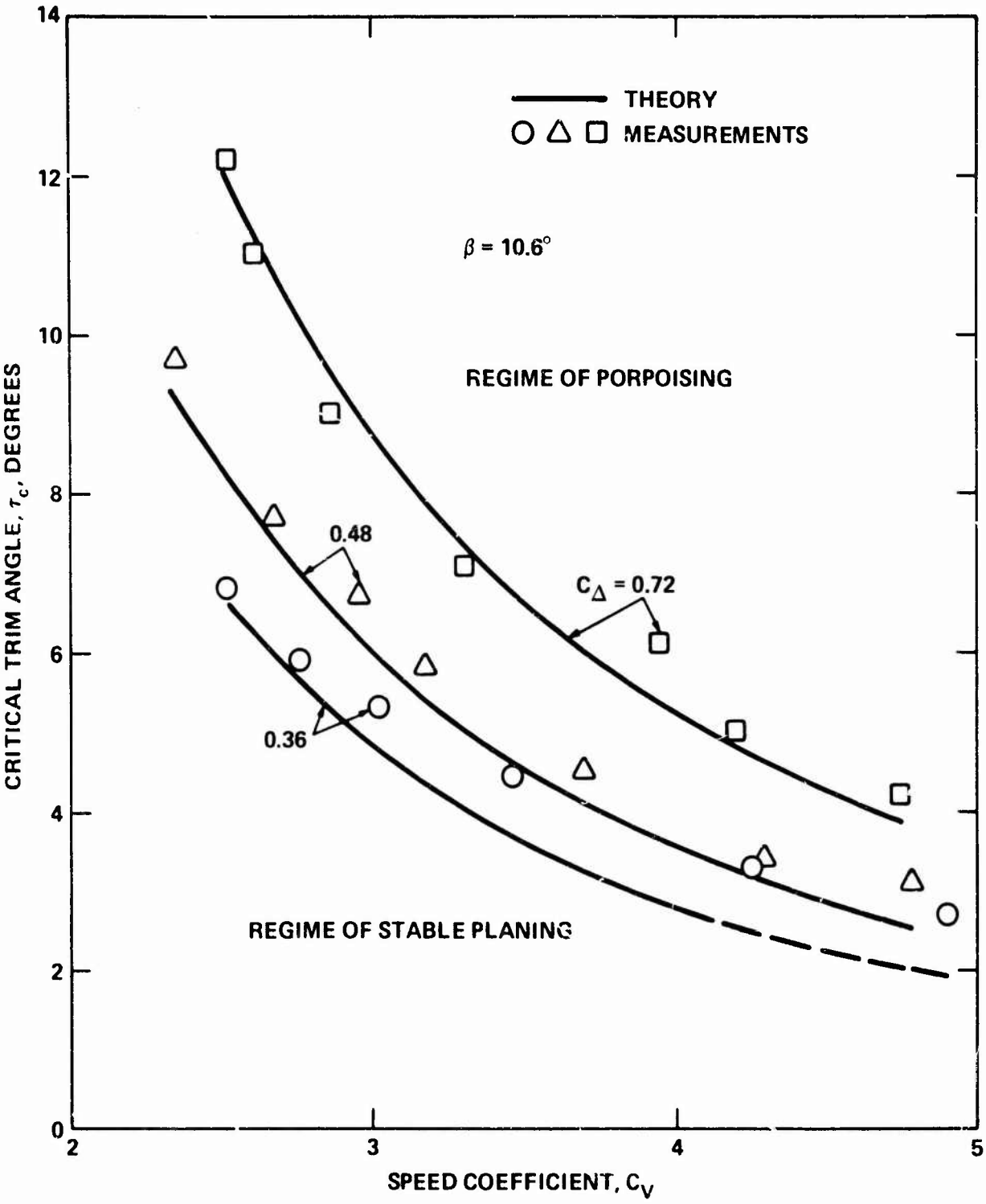

Figure 5 – Comparison of Theoretical and Measured Porpoising Boundaries for Deadrise of 10.6 Degrees

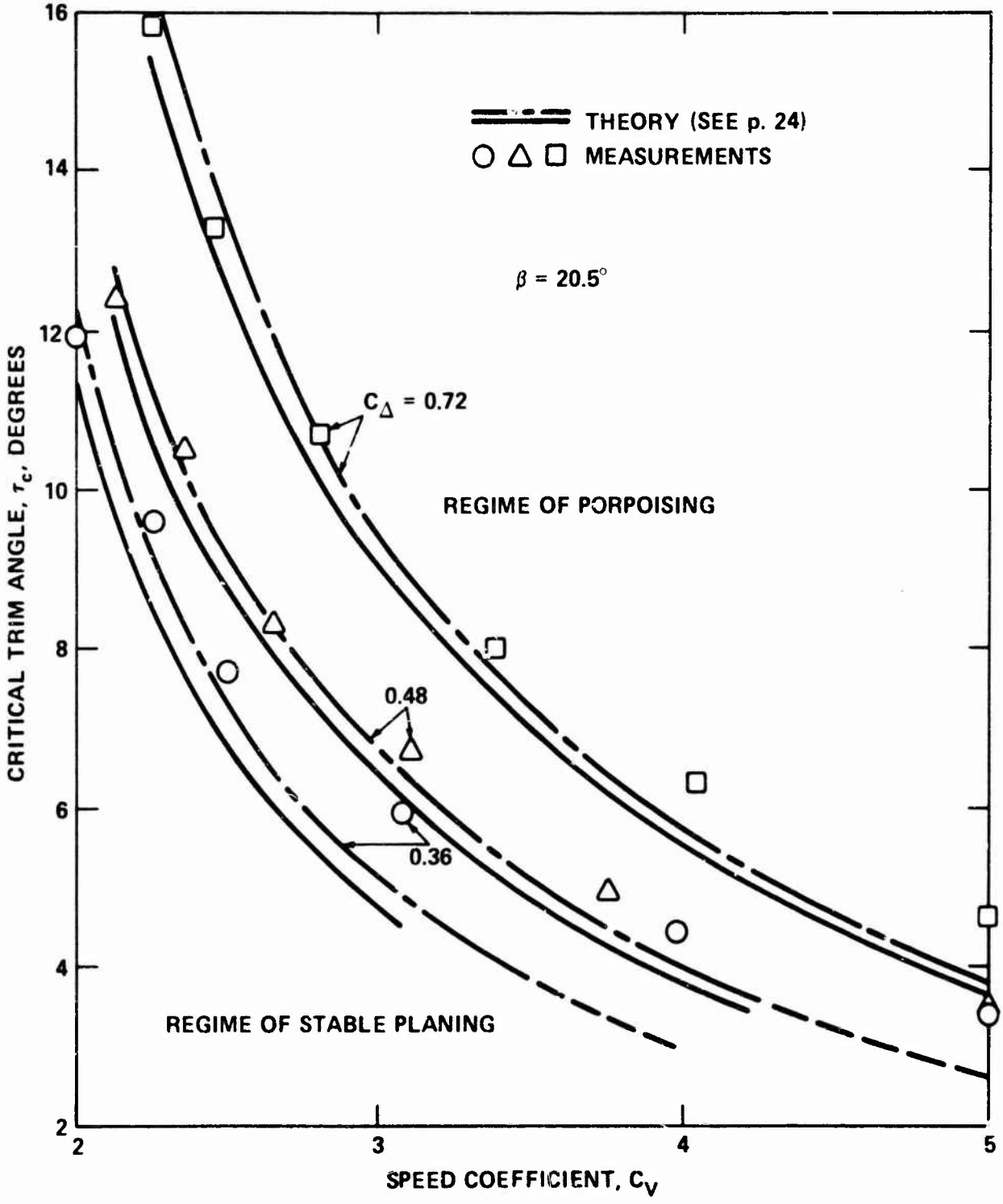

Figure 6 – Comparison of Theoretical and Measured Porpoising Boundaries for Deadrise of 20.5 Degrees

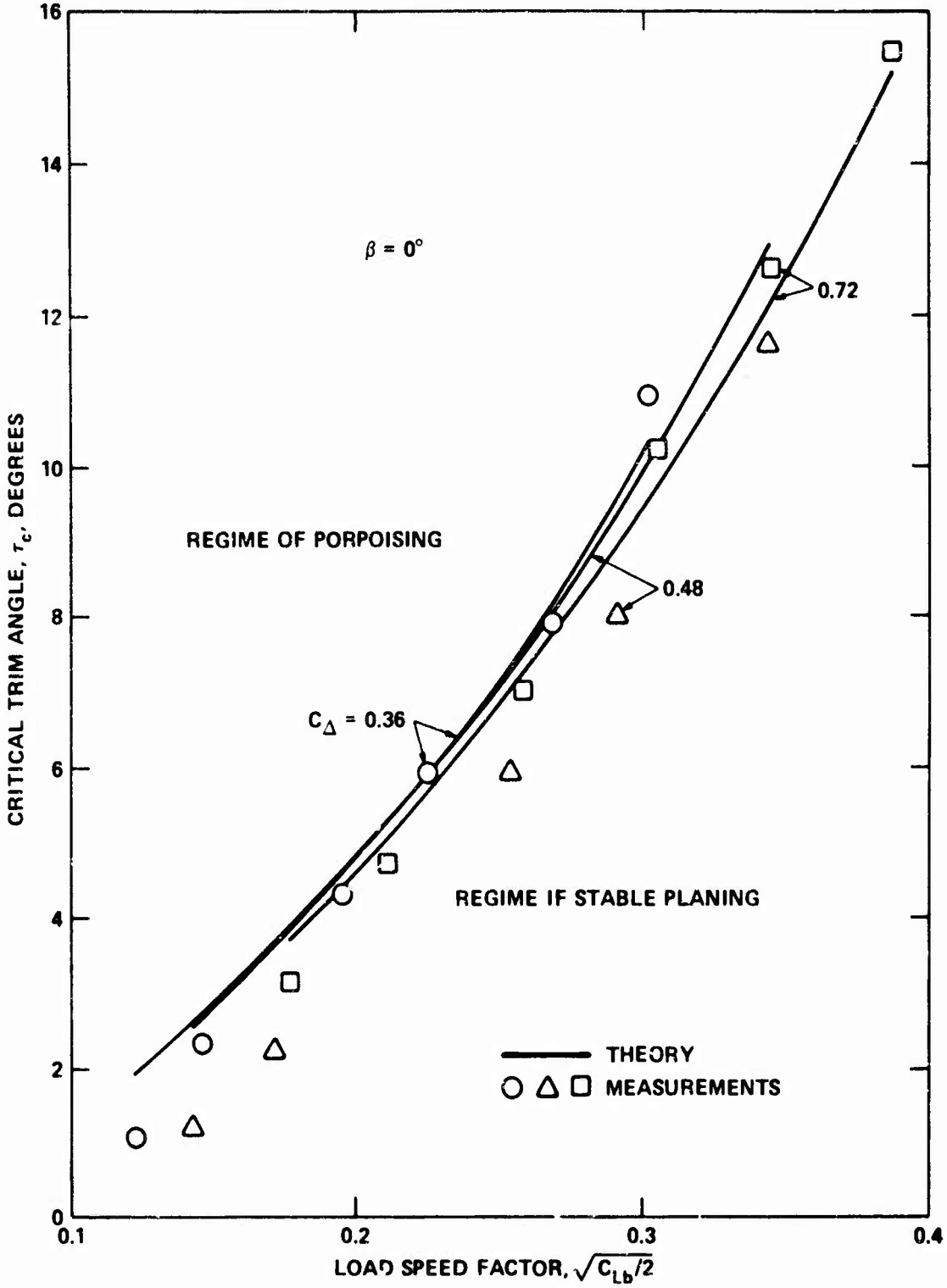

Figure 7 – Variation of Critical Trim Angle with Load Speed Factor for Various Loadings, Deadrise Angle of 0 Degrees

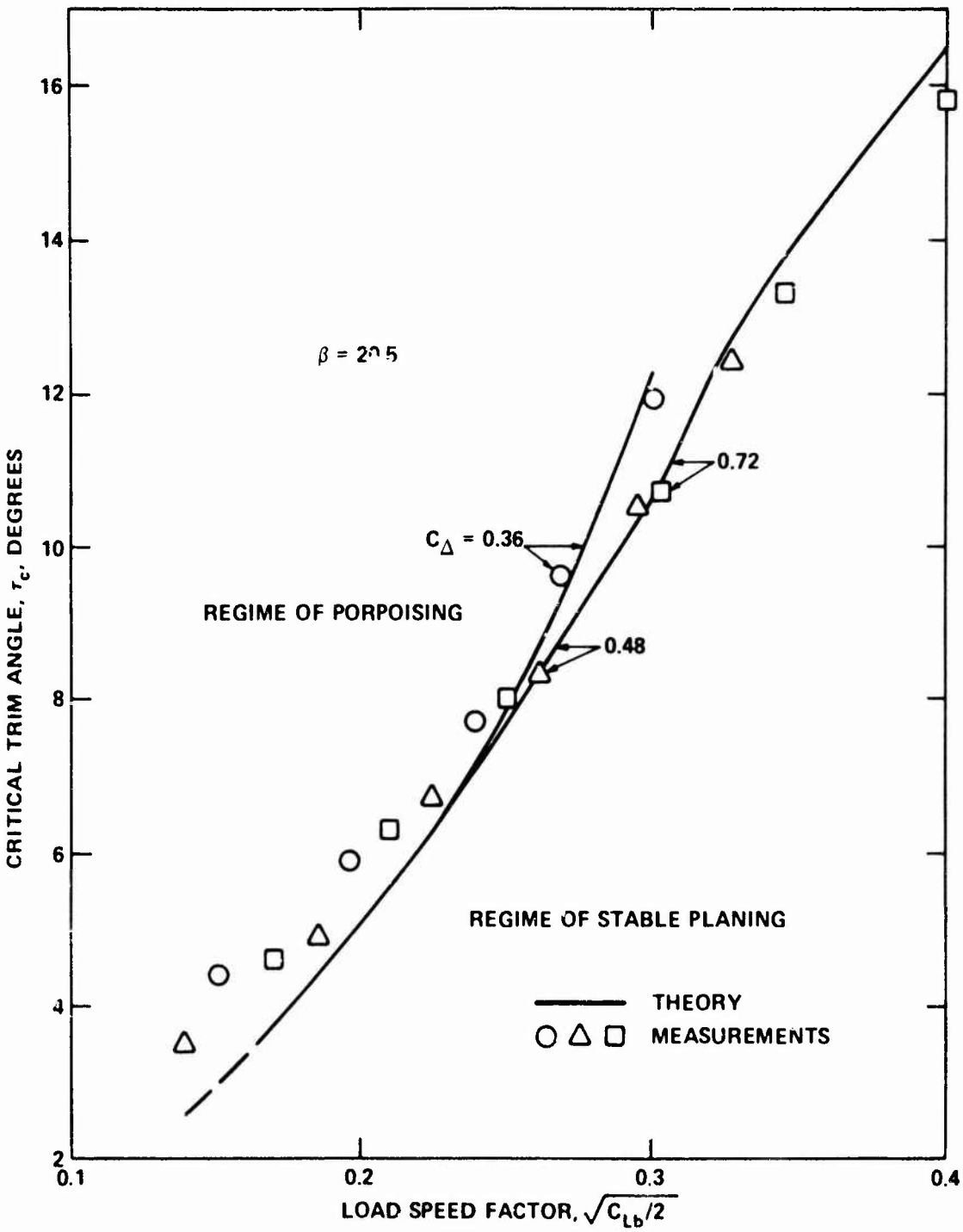

Figure 9 – Variation of Critical Trim Angle with Load Speed Factor for Various Loadings, Deadrise Angle of 20.5 Degrees

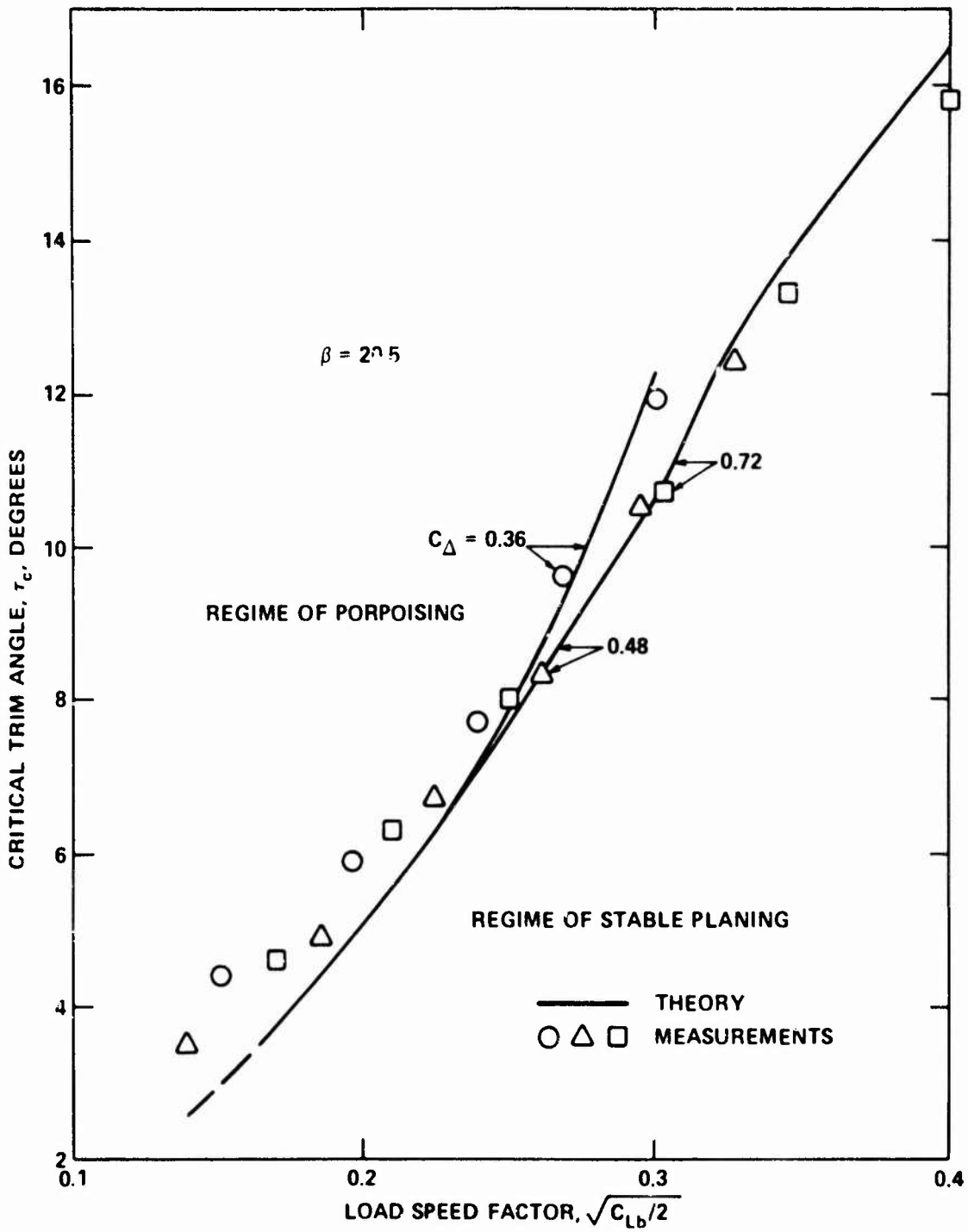

Figure 9 – Variation of Critical Trim Angle with Load Speed Factor for Various Loadings, Deadrise Angle of 20.5 Degrees

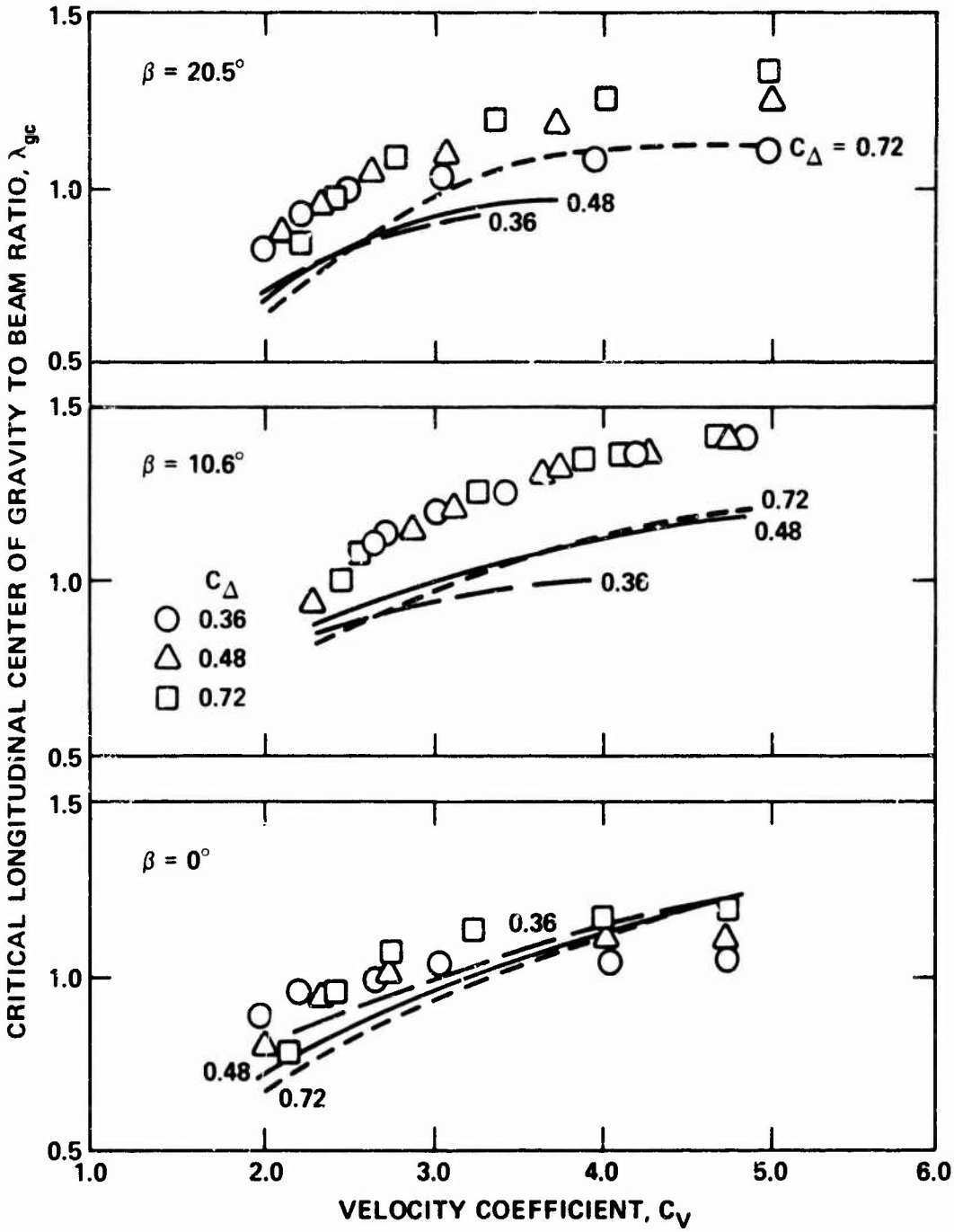

Figure 10 – Comparison of Measured with Computed Position of Center of Gravity at Porpoising

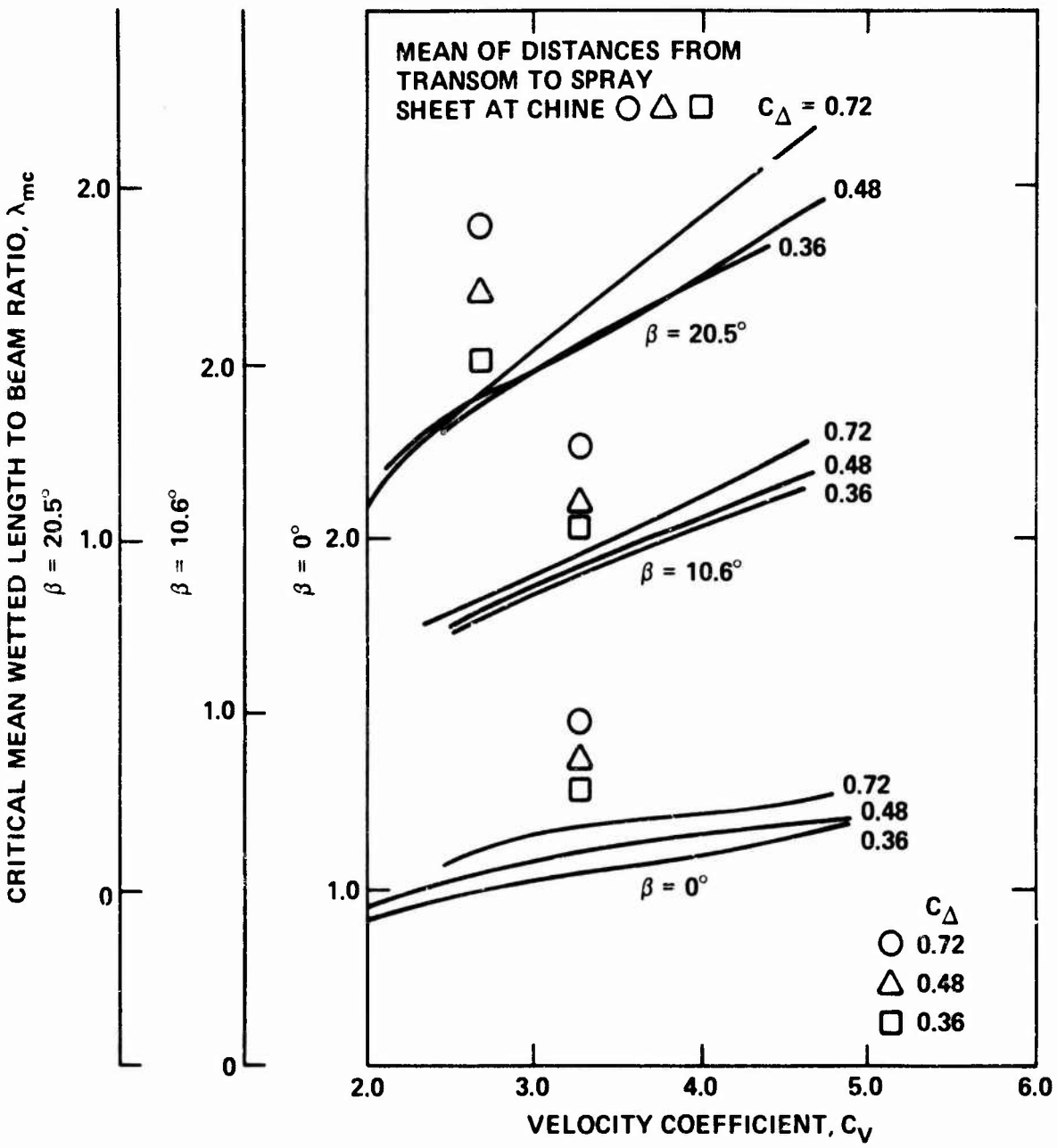

Figure 11 – Variation of Mean Wetted Length to Beam Ratio at Porpoising, with Speed, Deadrise Angle, and Loading

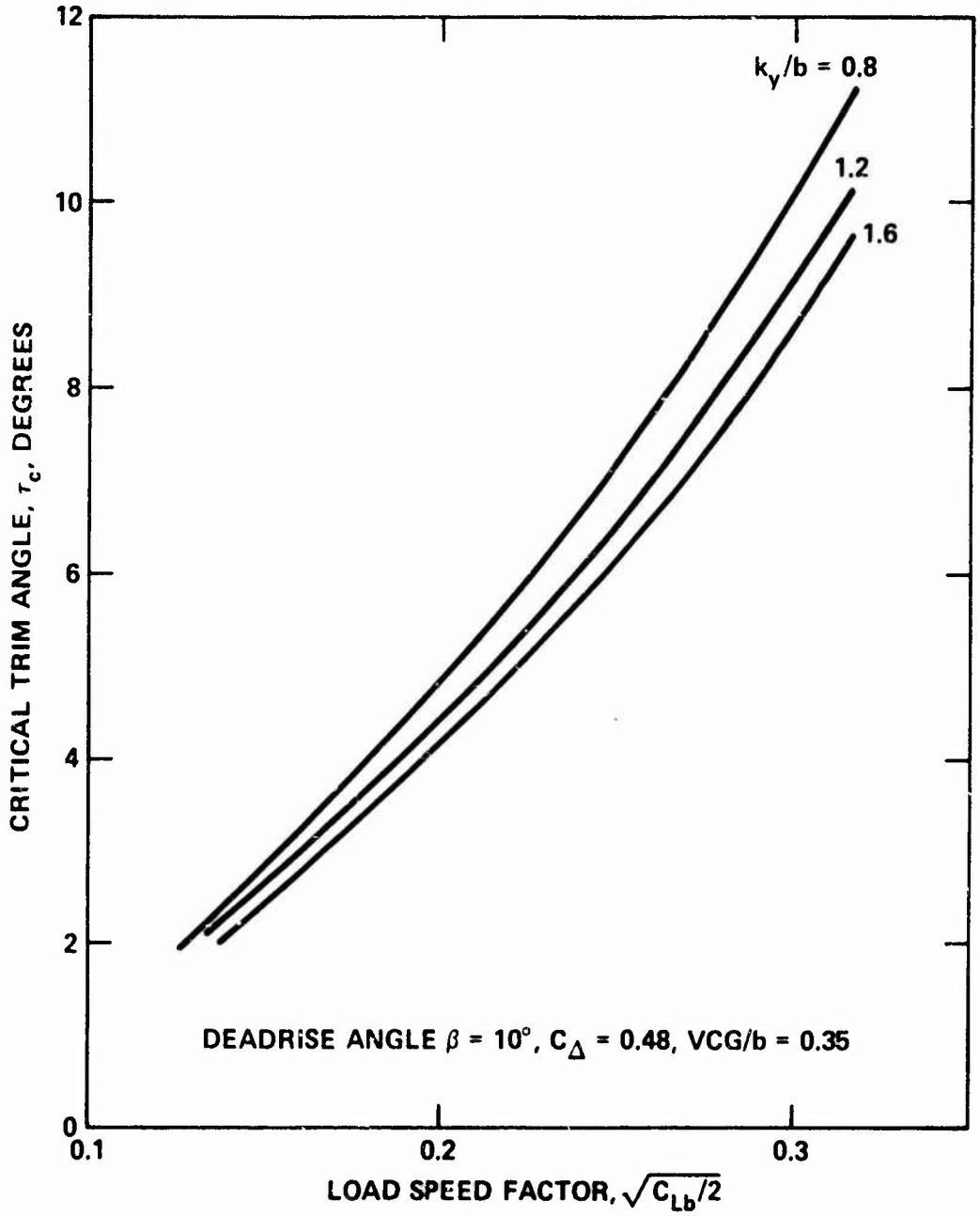

Figure 12 – Variation of Critical Trim Angle with Load Speed Factor and Radius of Gyration-Beam Ratio

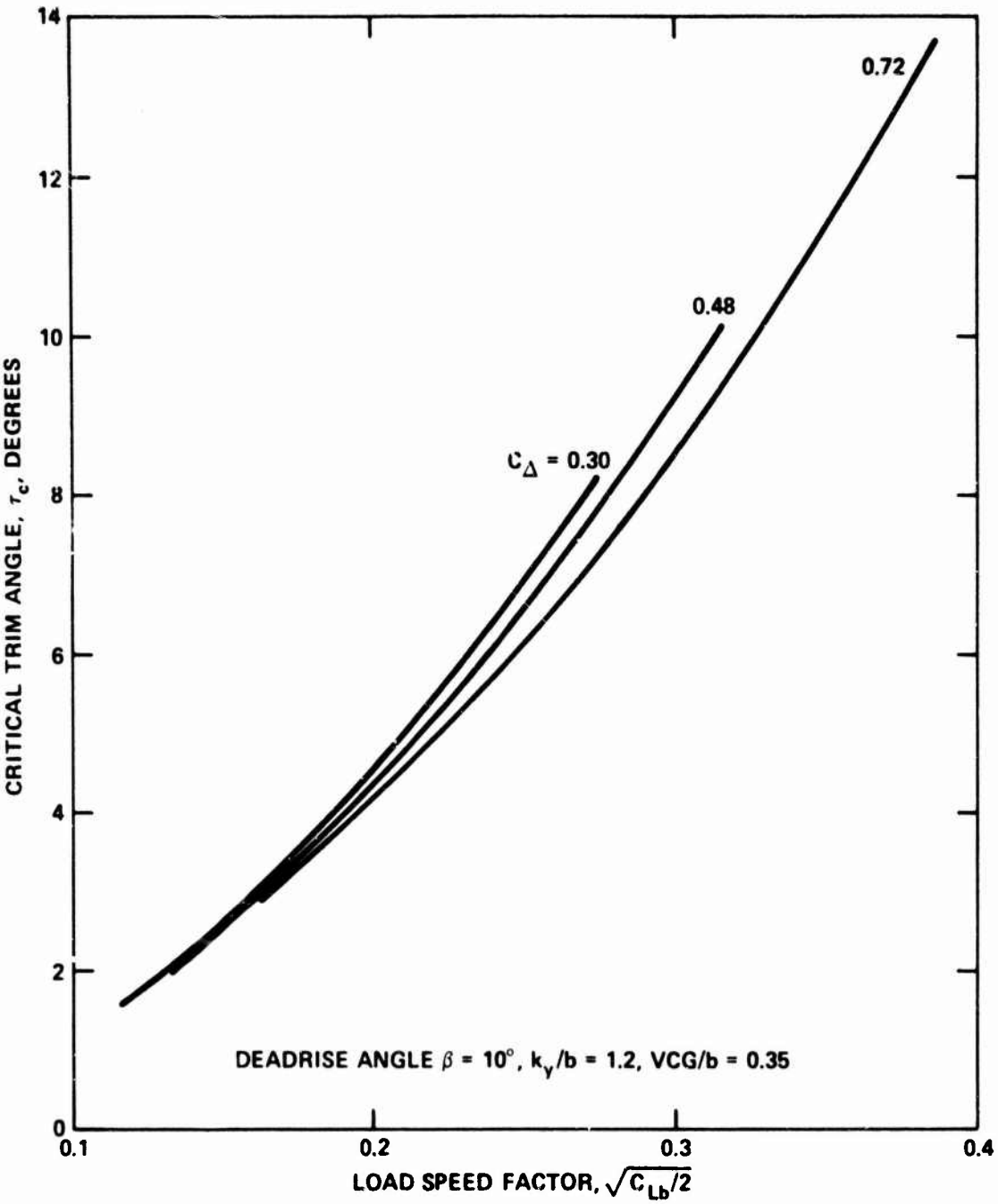

Figure 13 – Variation of Critical Trim Angle with Load Speed Factor and Load Coefficient

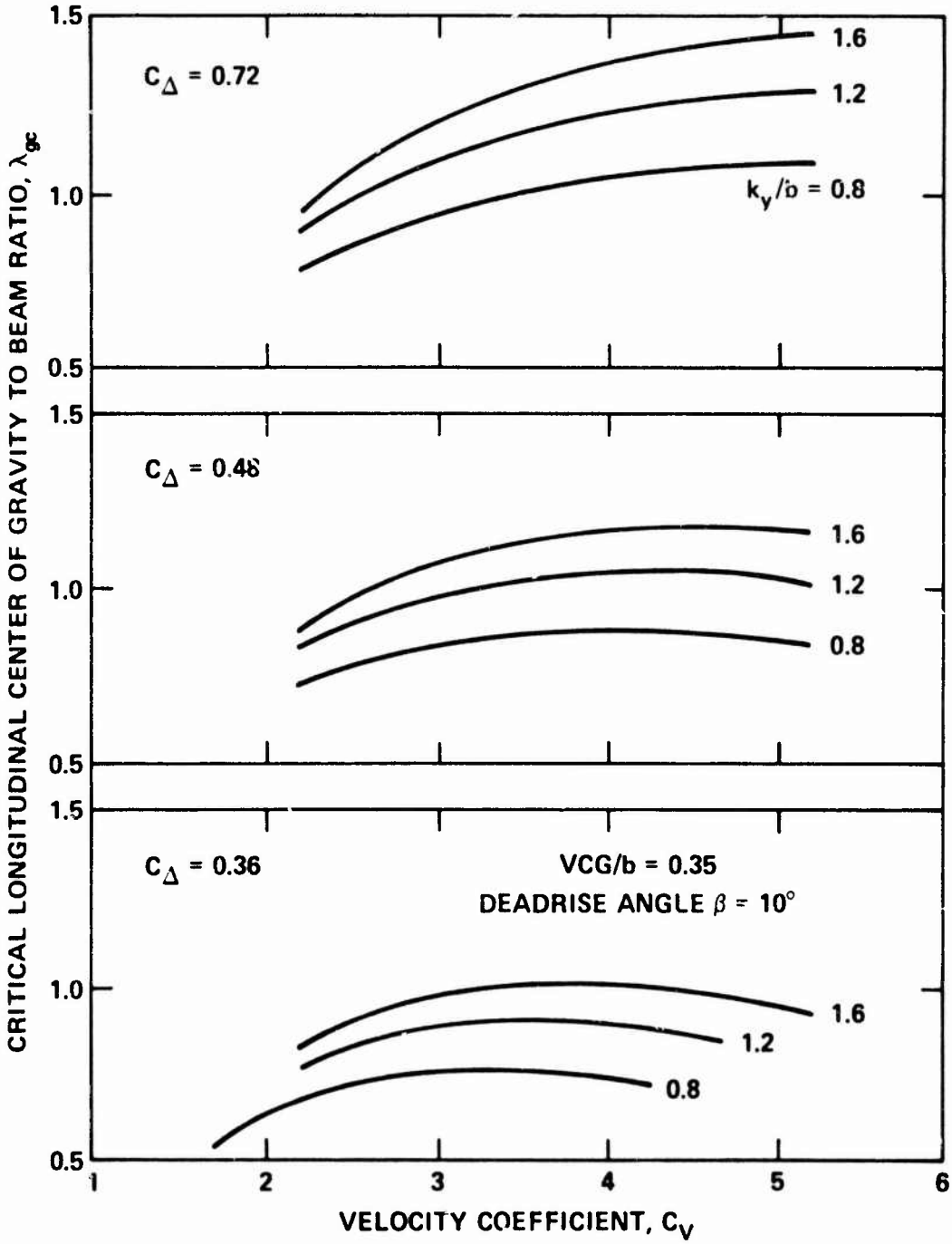

Figure 14 – Effect of Radius of Gyration and Speed on Location of Center of Gravity at Porpoising (Tow point at center of gravity)

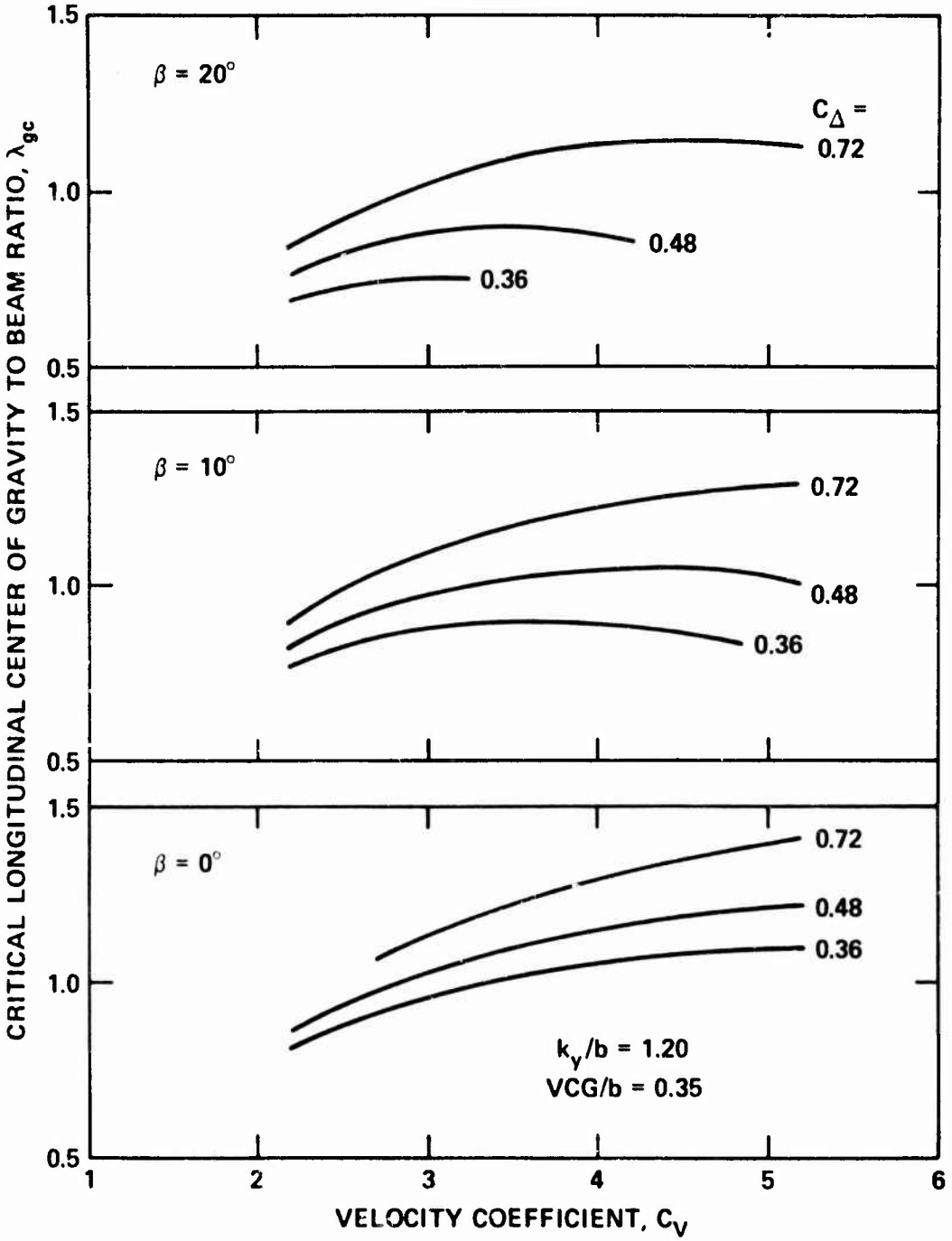

Figure 15 – Effect of Load Coefficient and Speed on Location of Center of Gravity at Porpoising (Tow point at center of gravity)

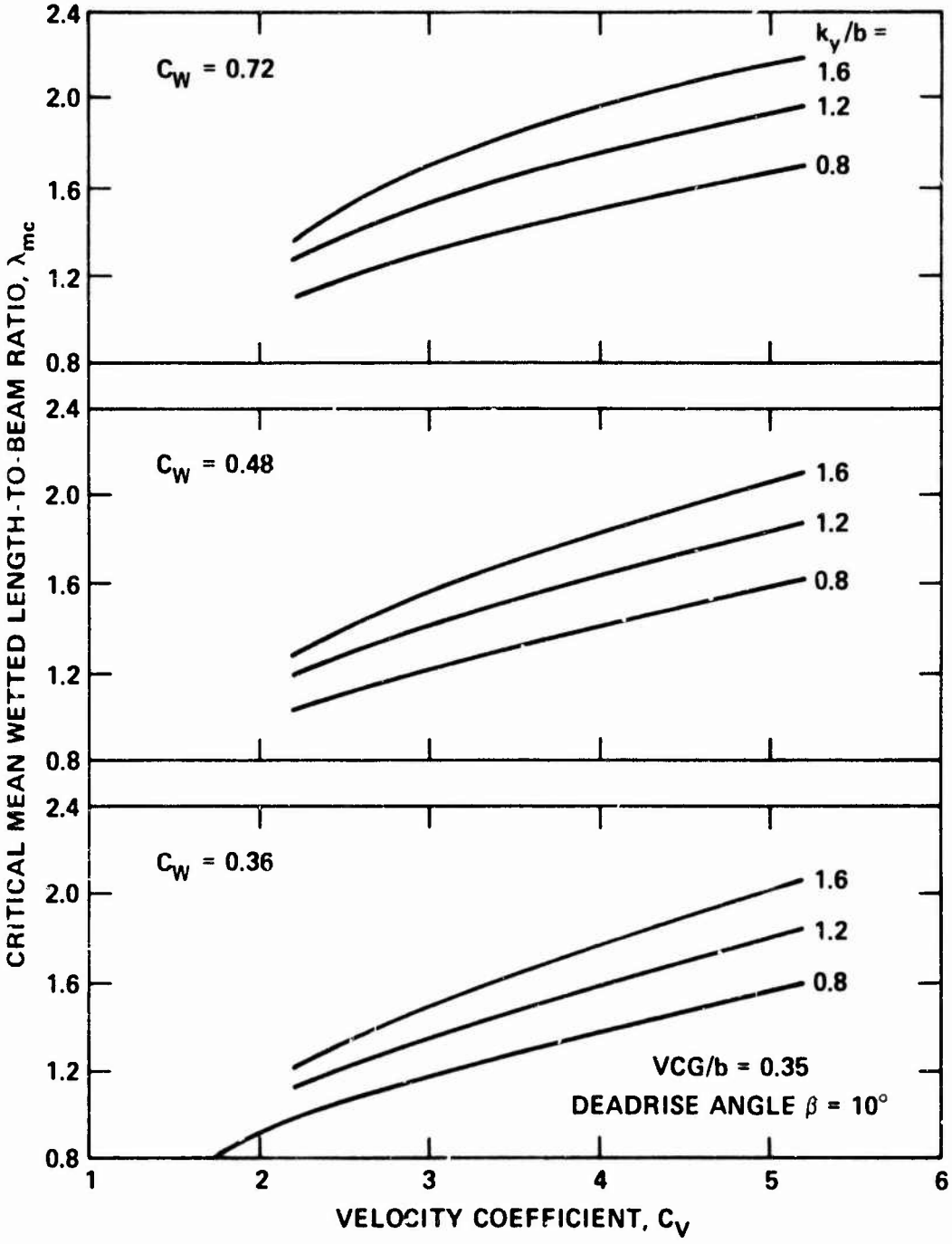

Figure 16 – Effect of Radius of Gyration and Speed on Mean Wetted Length at Porpoising (Tow point at center of gravity)

Figure 17 – Comparison of Theoretical Values of Critical Trim Angles with Davidson Laboratory Measurements

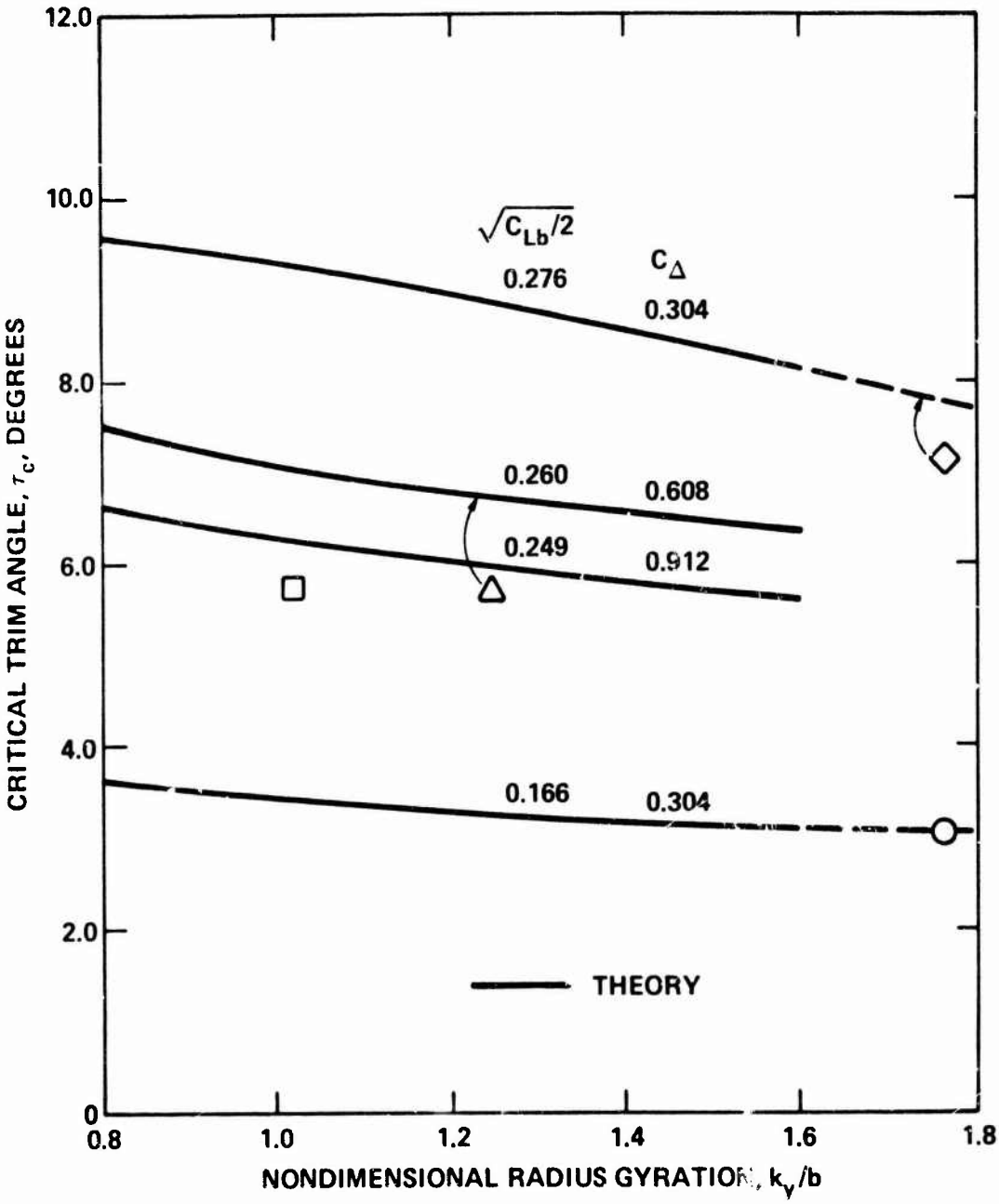

Figure 17a – Deadrise Angle $\beta = 10°$

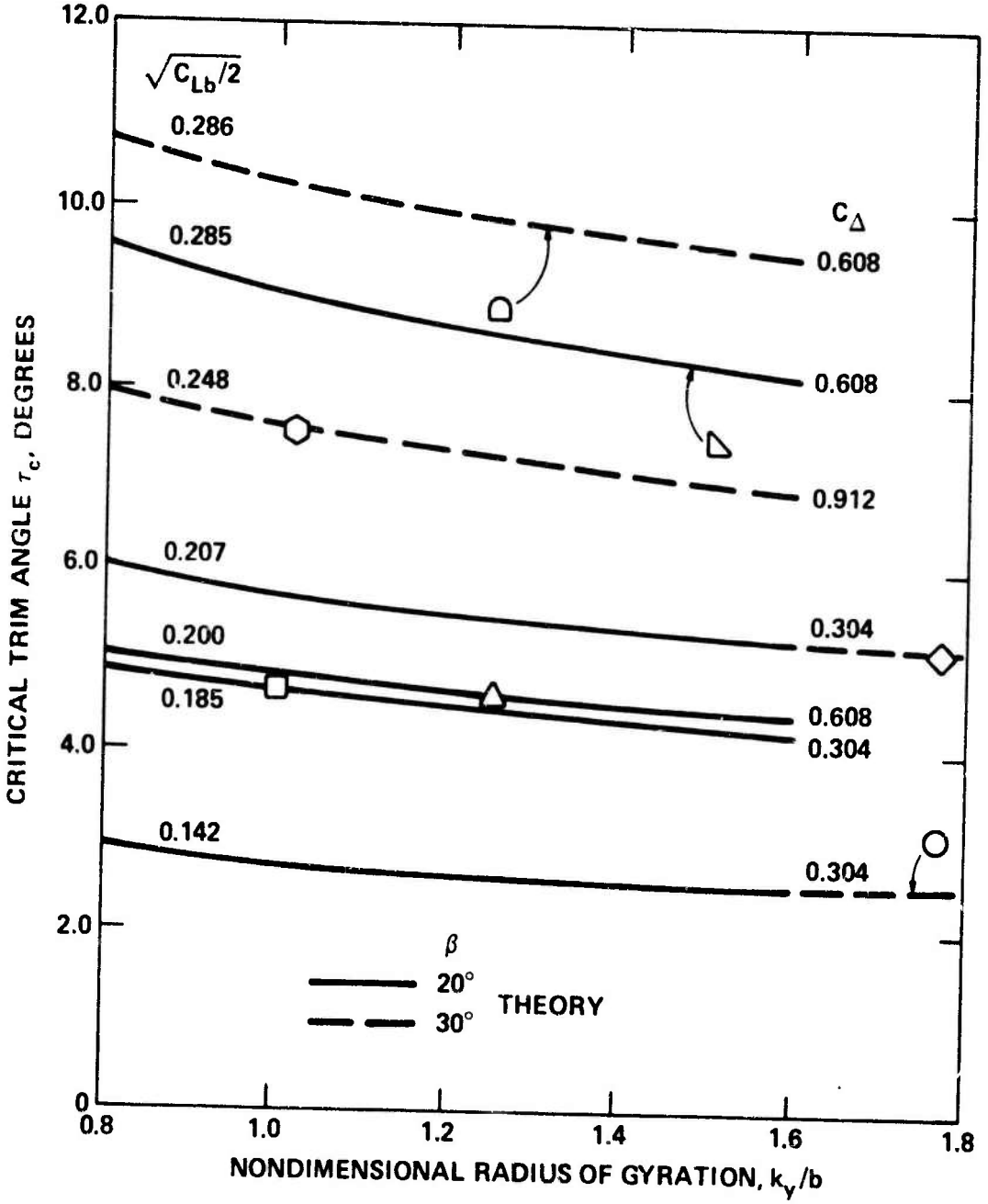

Figure 17b – Deadrise Angles, $\beta = 20°$ and $30°$

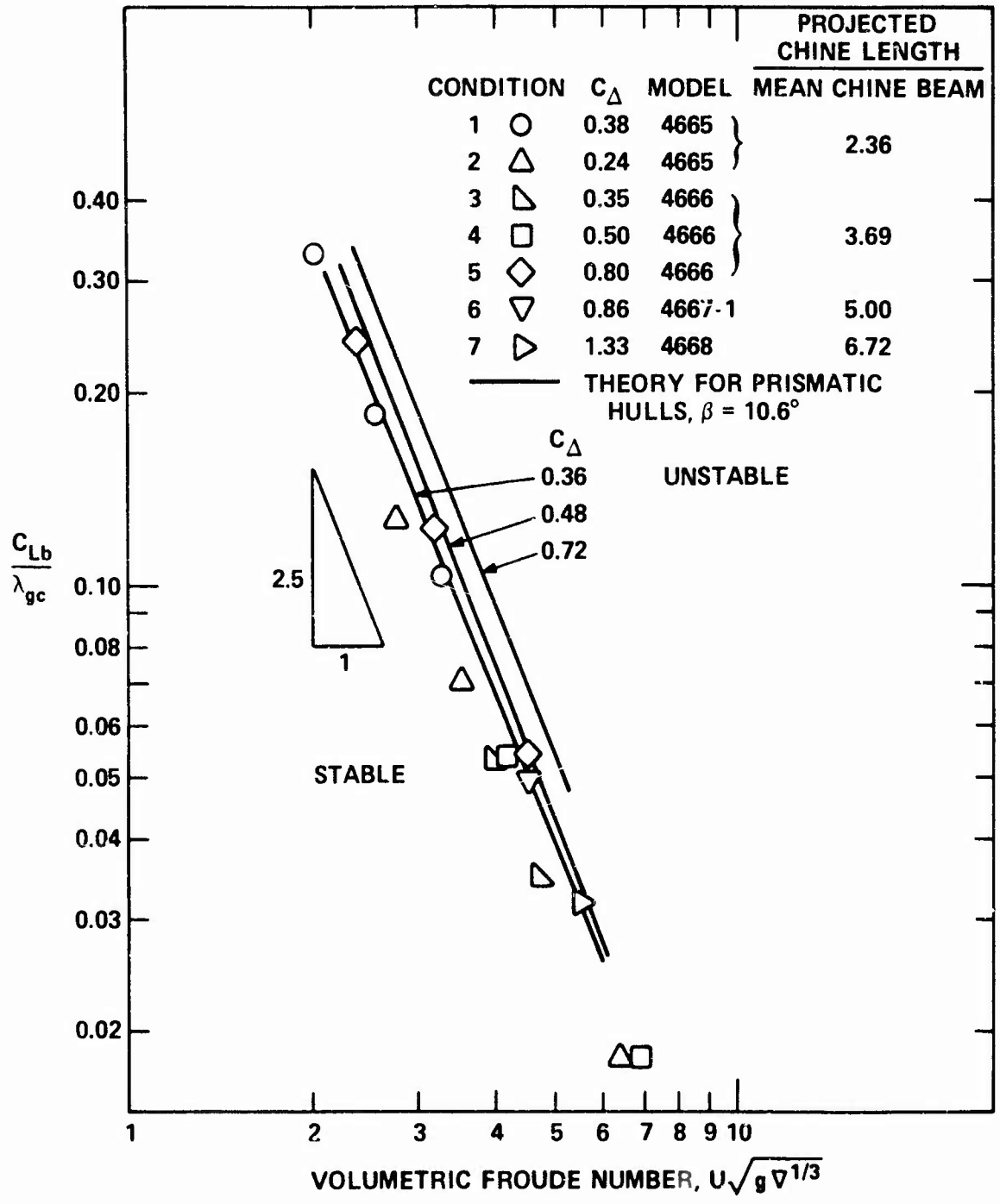

Figure 18 – Comparison of Approximate Estimates of Porpoising Boundaries of Reference 8 with DTMB Series 62 Model Data

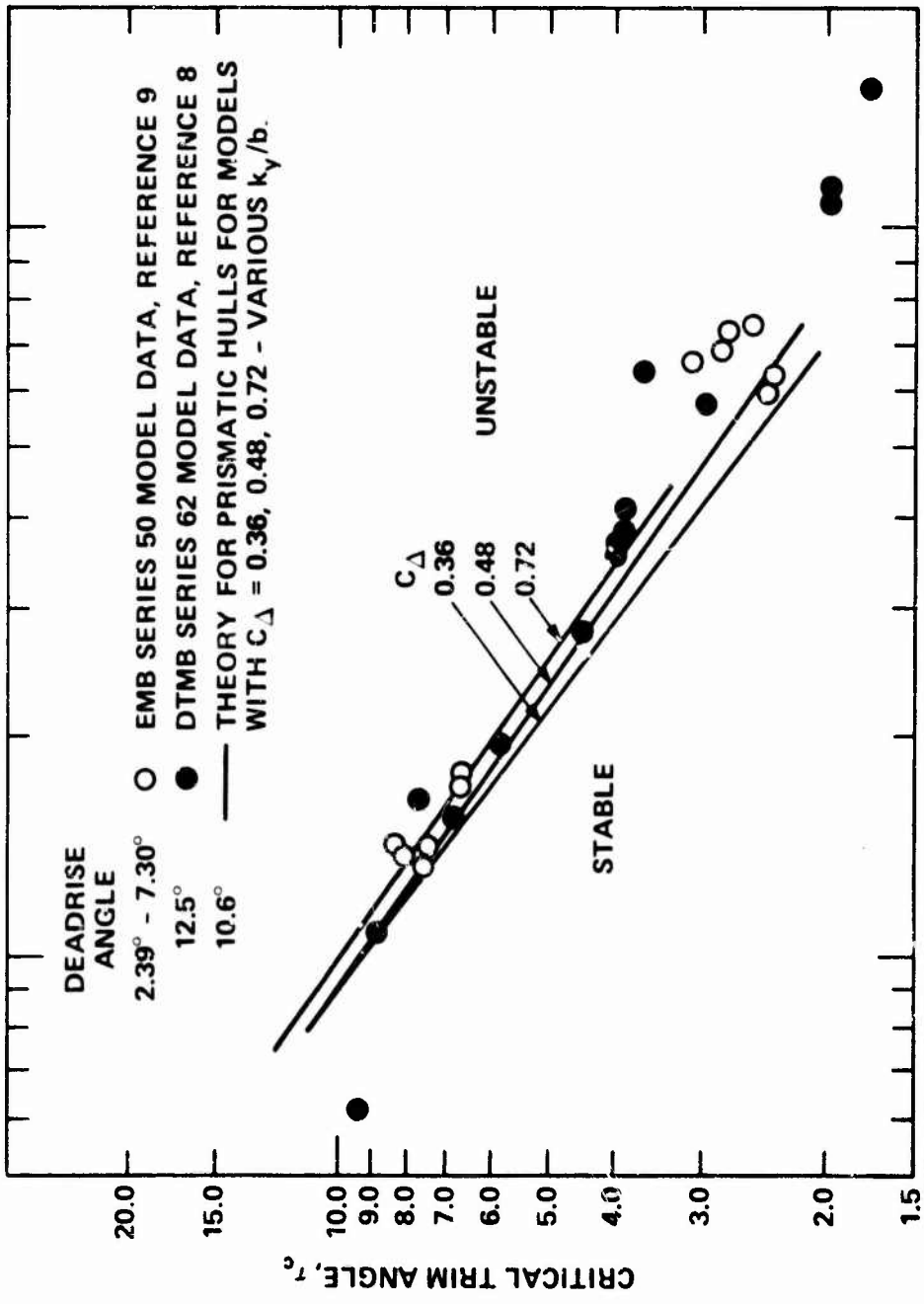

Figure 19 – Comparisons of Approximate Estimates of Porpoising Boundaries of Reference 11 with DTMB Series 62 and EMB Series 50 Model Data

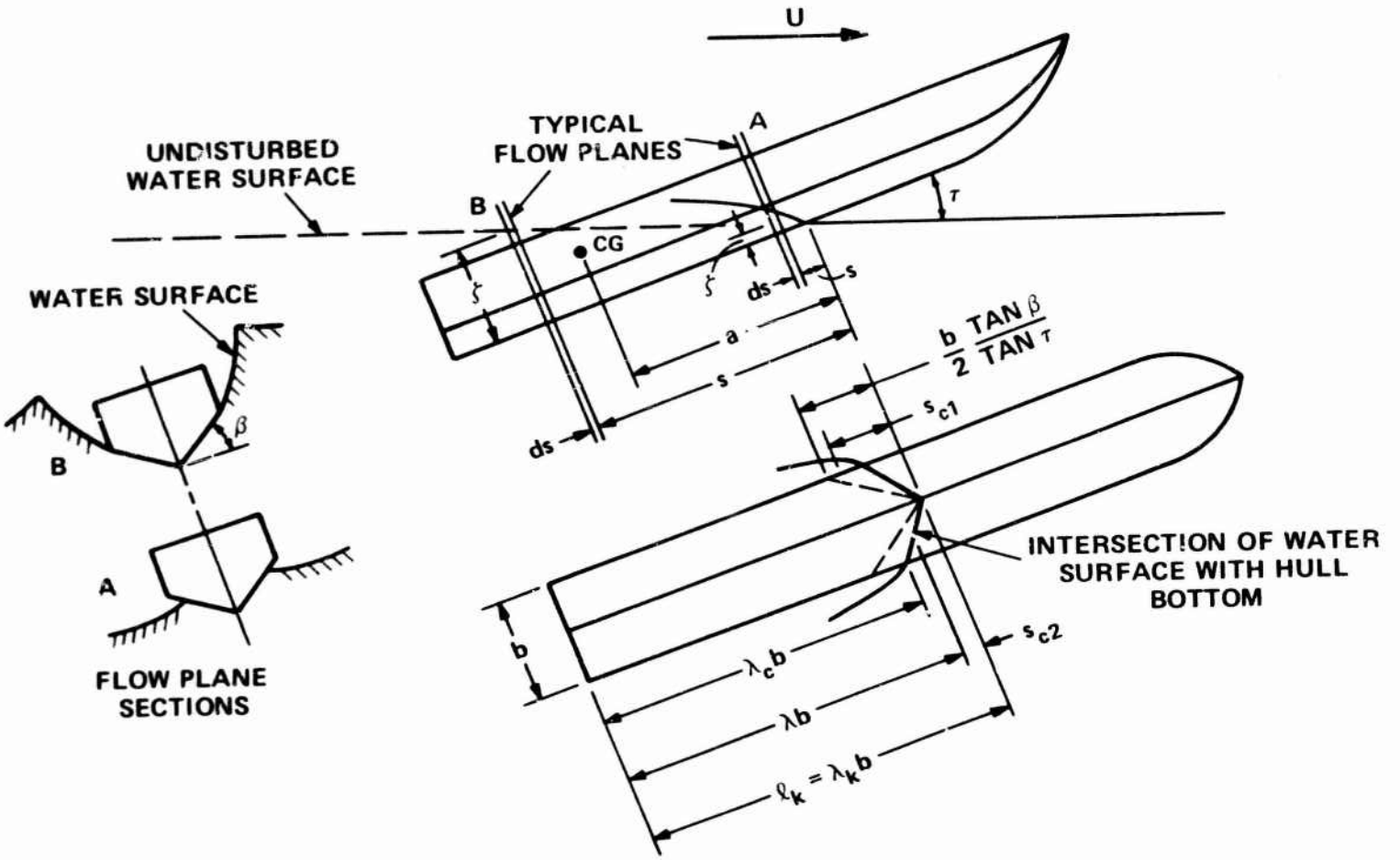

Figure 20 – Geometric Relationships in Steady State Planing

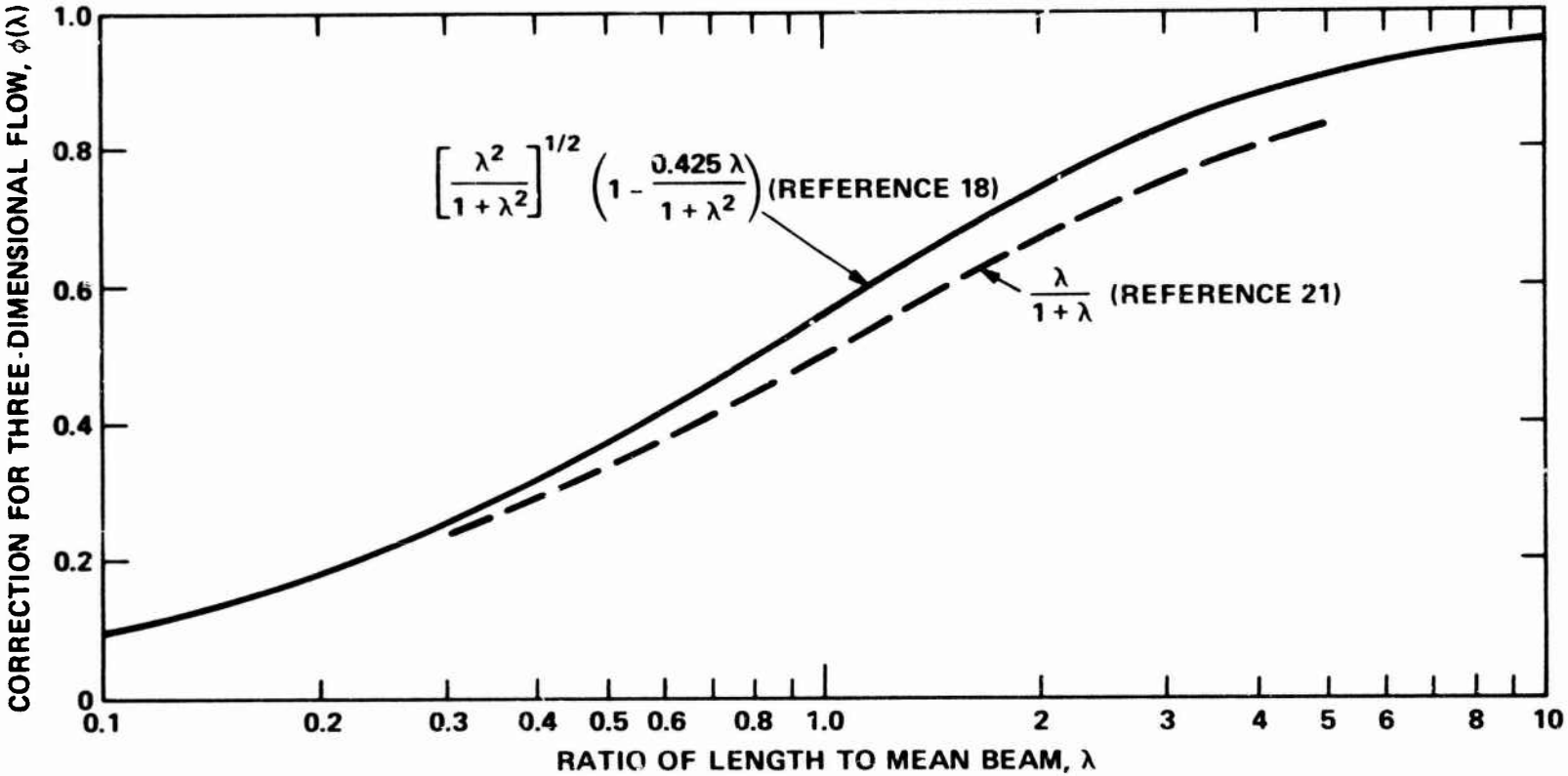

Figure 21 – Correction Factors for Three-Dimensional Flow

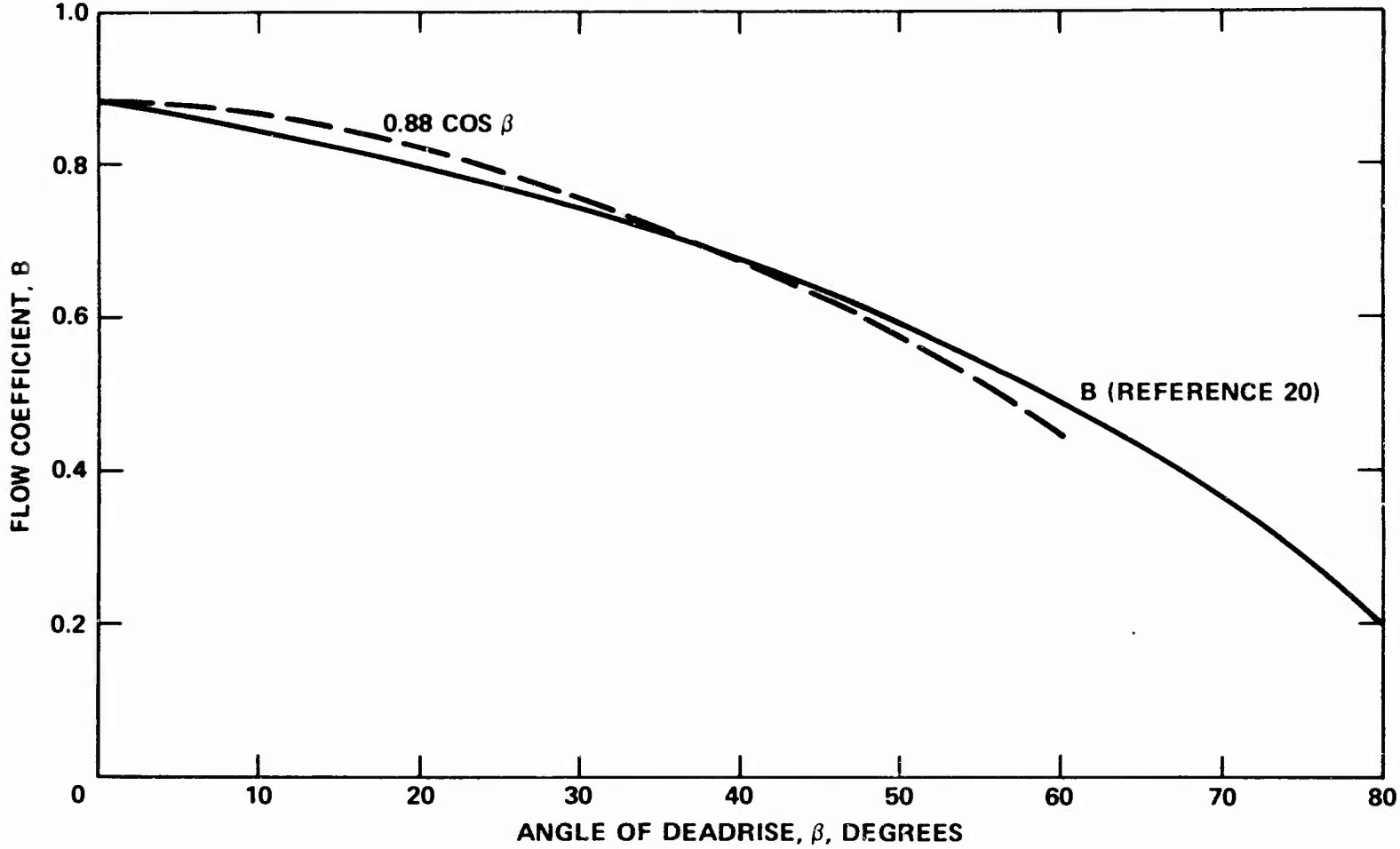

Figure 22 – Variation of Flow Coefficient with Deadrise Angle

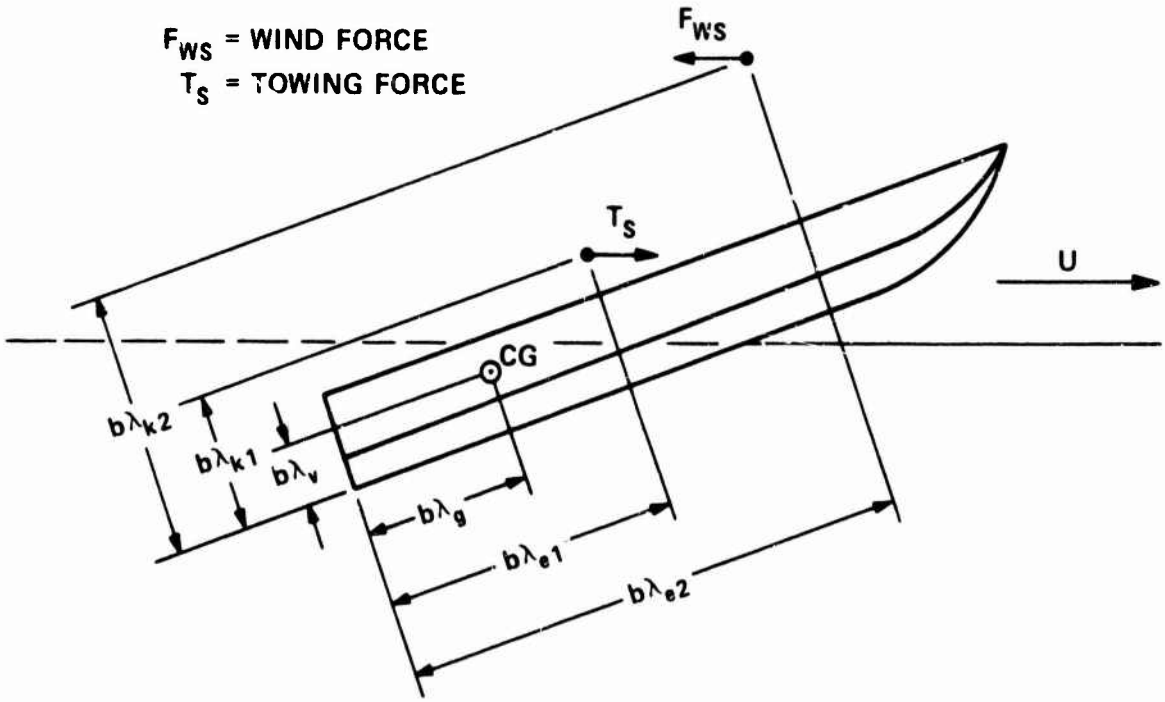

Figure 23 – Coordinates of Tow Point and Center of Wind Force

REFERENCES

1. Perring, W.G.A. and H. Glauert, "Stability on the Water of a Seaplane in the Planing Condition," Aeronautical Research Council, TR Vol. 42 (Sep 1933).

2. Lutowski, R.N., "A Computer Program for Various Performance Aspects of Planing Craft," Thesis submitted to Stevens Institute of Technology, Castle Point, Hoboken, N.J. (1973).

3. Payne, P.R., "Coupled Pitch and Heave Porpoising Instability in Hydrodynamic Planing," Journal of Hydronautics, Vol. 8, No. 2 (Apr 1974).

4. Day, J.P. and R.J. Haag, "Planing Boat Porpoising" Thesis Submitted to Webb Institute of Naval Architecture, Glen Cove, Long Island, N.Y. (May 1952).

5. Savitsky, D., "Hydrodynamic Design of Planing Hulls," Marine Technology, (Oct 1964).

6. Martin, M., "Theoretical Determination of Motion of High-Speed Planing Craft in Waves," DTNSRDC Report 76-0069 (Apr 1976).

7. Fridsma, G., "A Systematic Study of Rough-Water Performance of Planing Boats," Davidson Laboratory, Stevens Institute of Technology, Hoboken, N.J., Report 1275 (Nov 1969).

8. Clement, E.P. and D. Blount, "Resistance Tests of Systematic Series of Planing Hull Forms," Transactions Society of Naval Architects and Marine Engineers, Vol. 71, pp. 491-561 (1963).

9. Davidson, K.S.M. and A. Suarez, "Tests of Twenty Related Models of V-Bottom Motor Boats - EMB Series 50," David Taylor Model Basin Report R-47 (1949).

10. Brown, P.W., "An Experimental and Theoretical Study of Planing Surfaces with Trim Flaps," Davidson Laboratory, Stevens Institute of Technology, Hoboken, N.J., Report 1463 (Apr 1971).

11. Agnelli, J.C., "Evaluation of the Trim of a Planing Boat at Inception of Porpoising," presented at Spring Meeting of Society of Naval Architects and Marine Engineers, Lake Buena Vista, Fla. (Apr 1973).

12. Munk, M., "The Aerodynamic Forces on Airship Hulls," National Advisory Committee for Aeronautics Report 184 (1924).

13. Jones, R.T., "Properties of Low-Aspect-Ratio Wings at Speeds Below and Above the Speed of Sound," National Advisory Committee for Aeronautics Report 835 (1946).

14. Bryson, A.E., Jr., "Stability Derivatives for a Slender Missile with Application to a Wing-Body Vertical Tail Configuration," Journal of Aeronautical Sciences, Vol. 20, No. 5, pp. 297-308 (1953).

15. Mayo, W.L., "Analysis and Modification of Theory for Impact of Seaplanes on Water," National Advisory Committee for Aeronautics Report 810 (1945).

16. Milwitzky, B., "A Generalized Theoretical and Experimental Investigation of the Motions and Hydrodynamic Loads Experienced by V-Bottom Seaplanes During Step-Landing Impacts," National Advisory Committee for Aeronautics TN 1516 (1948).

17. Schnitzer, E., "Theory and Procedure for Determining Loads and Motions in Chine-Immersed Hydrodynamic Impacts of Prismatic Bodies," National Advisory Committee for Aeronautics Report 1152 (1953).

18. Pabst, W., "Landing Impact of Seaplanes," National Advisory Committee for Aeronautics TM 624 (1931).

19. Wagner, H., "The Phenomena of Impact and Planing on Water," National Advisory Committee for Aeronautics Translation 1366, ZAMM Bd 12, Heft 4, pp. 193-215 (Aug 1932).

20. Lamb, H., "Hydrodynamics," Sixth Edition, Cambridge University Press, England (1932).

21. Shuford, C.L., Jr., "A Theoretical and Experimental Study of Planing Surfaces Including Effects of Cross Section and Plan Form," National Advisory Committee for Aeronautics Report 1355 (1957).

22. Hadler, J.B., "The Prediction of Power Performance on Planing Craft," Transactions Society of Naval Architects and Marine Engineers, Vol. 74, pp. 563-610 (1966).

23. Ribner, H.S., "Propellers in Yaw," National Advisory Committee for Aeronautics Report 820 (1949).

24. Hsu, C.C., "On the Motions of High Speed Planing Craft," Hydronautics Report 603-1 (May 1967).

INITIAL DISTRIBUTION

Copies	
1	WES
1	CHONR/438 Cooper
2	NRL 1 Code 2027 1 Code 2629
1	ONR/Boston
1	ONR/Chicago
1	ONR/Pasadena
1	NORDA
4	USNA 1 Tech Lib 1 Nav Sys Eng Dept 1 B. Johnson 1 Bhattacheryya
3	NAVPGSCOL 1 Library 1 T. Sarpkaya 1 J. Miller
1	NADC
1	NELC/Lib
3	NUC, San Diego 1 Library 1 Fabula 1 Hoyt
1	NCSL/712 D. Humphreys
1	NCEL/Code 131
1	NSWC, Dahlgren
1	NUSC/Lib
7	NAVSEA 1 SEA 0322 1 SEA 033 1 SEA 03512/Peirce 1 SEA 037 3 SEA 09G32

Copies	
1	NAVFAC/Code 032C
1	NAVSHIPYD PTSMH/Lib
1	NAVSHIPYD PHILA/Lib
1	NAVSHIPYD NORVA/Lib
1	NAVSHIPYD CHASN/Lib
1	NAVSHIPYD LBEACH/Lib
2	NAVSHIPYD MARE 1 Library 1 Code 250
1	NAVSHIPYD BREM/Lib
1	NAVSHIPYD PEARL/Code 202.32
8	NAVSEC 1 SEC 6034B 1 SEC 6110 1 SEC 6114H 1 SEC 6120 1 SEC 6136 1 SEC 6140B 1 SEC 6144G 1 SEC 6148
1	NAVSEC, NORVA/6660.03 Blount
12	DDC
1	AFOSR/NAM
1	AFFOL/FYS, J. Olsen
1	NSF/Eng Lib
1	LC/Sci & Tech
1	DOT/Lib TAD-491.1
2	MMA 1 Capt McCready 1 Library
1	U. of Bridgeport/E. Uram

Copies	
4	U. of Cal/Dept Naval Arch, Berkely
	1 Library
	1 Webster
	1 Paulling
	1 Wehausen
2	U. of Cal, San Diego
	1 A. T. Ellis
	1 Scripps Inst Lib
3	CIT
	1 Aero Lib
	1 T. Y. Wu
	1 A. Acosta
1	City College, Wave Hill/Pierson
1	Catholic U. of Amer./Civil & Mech Eng
1	Colorado State U./Eng Res Cen
1	U. of Connecticut/Scottron
1	Cornell U./Sears
2	Florida Atlantic U.
	1 Tech Lib
	1 S. Dunne
2	Harvard U.
	1 G. Carrier
	1 Gordon McKay Lib
1	U. of Hawaii/Bretschneider
1	U. of Illinois/J. Robertson
3	U. of Iowa
	1 Library
	1 Landweber
	1 Kennedy
1	Johns Hopkins U./Phillips
1	Kansas State U./Nesmith
1	U. of Kansas/Civil Eng Lib
1	Lehigh U./Fritz Eng Lab Lib

Copies	
5	MIT
	1 Library
	1 Leehey
	1 Mandel
	1 Abkowitz
	1 Newman
4	U. of Minn/St. Anthony Falls
	1 Silberman
	1 Schiebe
	1 Wetzel
	1 Song
3	U. of Mich/NAME
	1 Library
	1 Ogilivie
	1 Hammitt
2	U. of Notre Dame
	1 Eng Lib
	1 Strandhagen
2	New York U./Courant Inst
	1 A. Peters
	1 J. Stoker
1	Penn State/Arl/B. Parkin
1	Princeton U./Mellor
5	SIT
	1 Library
	1 Breslin
	1 Savitsky
	1 P. W. Brown
	1 Fridsma
1	U. of Texas/Arl Lib
1	Utah State U./Jeppson
2	Southwest Res Inst
	1 Applied Mech Rev
	1 Abramson
2	Stanford U.
	1 Eng Lib
	1 R. Street

Copies	
1	Stanford Res Inst/Lib
1	U. of Washington/Arl Tech Lib
3	Webb Inst
	1 Library
	1 Lewis
	1 Ward
1	Woods Hole/Ocean Eng
1	Worchester PI/Tech Lib
1	SNAME/Tech Lib
1	Bethlehem Steel/Sparrows Point
1	Bethlehem Steel/New York/Lib
1	Bolt, Beranek & Newman/Lib
1	Exxon, NY/Design Div, Tank Dept
1	General Dynamics, EB/Boatwright
1	Gibbs & Cox/Tech Info
5	Hydronautics
	1 Library
	1 E. Miller
	1 A. Goodman
	1 V. Johnson
	1 C. C. Hsu
1	Lockheed, Sunnyvale/Waid
2	McDonnell Douglas, Long Beach
	1 J. Hess
	1 T. Cebeci
1	Newport News Shipbuilding/Lib
1	Nielsen Eng & Res
1	Oceanics
1	Rockwell International/B. Ujihara
1	Sperry Rand/Tech Lib
1	Sun Shipbuilding/Chief Naval Arch

Copies	
1	Robert Taggart
1	Tracor

CENTER DISTRIBUTION

Copies	Code	
1	1500	W. E. Cummins
1	1504	V. J. Monacella
1	1506	M. K. Ochi
1	1507	D. Cieslowski
1	1512	J. B. Hadler
1	1520	R. Wermter
1	1521	P. Pien
1	1524	Y. T. Shen
1	1524	W. C. Lin
1	1532	G. Dobay
1	1532	R. Roddy
1	1540	W. B. Morgan
1	1552	J. McCarthy
1	1552	N. Salvesen
1	1560	G. Hagen
1	1560	N. Hubble
10	1562	M. Martin
1	1564	J. Feldman
1	1568	G. Cox
1	1572	M. D. Ochi
1	1572	E. Zarnick
1	1572	C. M. Lee
1	1576	W. E. Smith
30	5214.1	Reports Distribution
1	5221	Unclassified Library (C)
1	5222	Unclassified Library (A)